Figure 4 Venn-diagram selection of LH- and antidepressant-associated transcripts in the frontal cortex (a) and hippocampus (b). Comparisons were made between control ($n = 6$) and LH-S rats ($n = 6$), between LH-S and LH-F rats ($n = 5$), and between LH-S and LH-I rats ($n = 5$). The LH-I and LH-F rats were those that showed more than 50% success in escape behavior after drug treatments. The number in each compartment denotes the number of differentially expressed transcripts between two groups (see Materials and Methods for a definition of our criteria).

increased after initiating therapy. Approximately 38% of LH-associated transcripts in the FC and 56% in the HPC could not be normalized by either antidepressant (Figure 4; red area). These transcripts could represent the potential targets for novel antidepressants with efficacy against refractory depression. The green, purple and light blue segments in Figure 4 depict the transcripts with expression levels that did not differ between control and LH-S groups, but were significantly altered by fluoxetine, imipramine or both drug treatments, respectively. The information on these transcripts is provided as supplementary Tables S1 and S2. Some of these transcripts may be relevant to the manifestation of adverse reactions by TCA and SSRI. Tables 1 and 2 show the listing of LH-associated transcripts according to putative functions, along with P-values between different treatment groups. Data are also provided on the 'average difference' $\pm$SE of each transcript (that corresponds to an absolute value) in supplementary Tables S1 and S2. In all, 17 known genes and one EST showed downregulation (marked in red), whereas 16 transcripts including ESTs were upregulated in the FC (Table 1). In contrast, the majority of known LH-associated genes in the HPC were downregulated (27 of 31) (marked in red in Table 2). Even allowing for ESTs, the number of downregulated transcripts in the HPC significantly exceeds the upregulated transcripts (32 vs 16) (Table 2).

We chose four genes from each of Tables 1 and 2, and examined mRNA levels in the same RNA samples used for microarray experiments under 'one-step' quantitative RT-PCR reactions (Table 3). These results showed the same direction of expressional changes seen in the microarray experiments, but less correlation was found with the degree of change between the two methods, as indicated in prior studies.[25,26] Furthermore, since only a limited number of transcripts were confirmed by independent methods and no

transcripts were confirmed when Bonferroni's correction was applied to the quantitative RT-PCR results, the present DNA microarray data are broadly unconfirmed.

LH-associated Transcripts in the FC

When classified according to function, genes defined as receptors or ion channel/transporters were all downregulated in LH animals (Table 1). Among them, the serotonin receptor type 2A (Htr2a) gene showed a 1.6-fold decrease, and recovery with both fluoxetine and imipramine. Evidence from other animal models for depression[27,28] and clinical observations[29] have also suggested a pathological role for HTR2A in the depressive state. The change in inositol-1,4,5-triphosphate receptor type 1 (Itpr1) level was small, but statistically significant. Both types of antidepressant normalized the reduced expression of Itpr1. The observed decrease in both Htr2a and Itpr1 and their restitution to original levels by antidepressants is in keeping with a proposed theory of dysregulated monoamine-mediated calcium signaling in depression.[30,31] Other members of the receptor and ion channel/transporter gene families that showed restoration with fluoxetine or imipramine included a voltage-gated potassium channel and zinc transporter (Table 1). Conversely, three genes from the signal transduction family were all upregulated in LH-S rats compared to controls (Table 1). Of interest is prostaglandin D synthase, an enzyme that produces prostaglandin D_2, a potent endogenous sleep-promoting substance.[32] This enzyme has recently been implicated in the regulation of nonrapid eye movement (NREM).[33] Sleep disturbance is a typical symptom of human depression. Examination of sleep parameters in LH rats, particularly the NREM period, would therefore be of interest. Protein kinase C epsilon (PKCε), which is a member of nPKC, showed a small but significant increase in LH-S compared with controls.

Table 1 LH-associated transcripts in the frontal cortex

Functional Groups	Fold change[a]	P-value[b]			Accession no.
		Cont vs LH-S	LH-S vs LH-F	LH-S vs LH-I	
Receptor					
Inositol-1,4,5-triphosphate receptor type I	−1.1	0.0032	0.0078	0.0078	J05510
Serotonin receptor 2A	−1.6	0.0479	0.0352	0.0358	M64867
Ion channel/Transporter					
Voltage-gated potassium channel	−1.1	0.0289	0.0078		X62840
Dri 27/ZnT4 (zinc transporter)	−1.3	0.0289		0.0026	Y16774
Cl-/HCO3- exchanger (B3RP2)	−1.4	0.0484			J05166
Signal transduction					
Prostaglandin D2 synthetase	1.3	0.0484	0.0006	0.0181	J04488
PKC epsilon	1.2	0.0158	0.0181		M18331
Neurexophilin 4	2.0	0.0156			AF042714
Neural growth/ structure					
Tau	−1.1	0.0479	0.0358		X79321
Jagged2 precursor	1.3	0.0158		0.0358	U70050
Similar to cdc37	1.6	0.0484			D26564
MAP2	−1.4	0.0158			S74265
H36-alpha7 integrin alpha chain	−1.5	0.0289			X65036
Neu differentiation factor	−1.6	0.0484			M92430
LIMK-1	−9.5	0.0436			D31873
Metabolic enzymes					
Thioradoxin reductase 1	−1.2	0.0011	0.0181		AA891286
F1-ATPase epsilon subunit	1.1	0.0011		0.0026	AI171844
Mitochondrial fumarase	−1.1	0.0110		0.0181	J04473
Lipoprotein lipase	1.5	0.0484			L03294
24-kDa subunit of mitochondrial NADH dehydrogenase	1.4	0.0484			M22756
Bleomycin hydrolase	1.4	0.0158			D87336
Stress response					
Rapamycin and FKBP12 target-1 protein (rRAFT1)	1.1	0.0158	0.0358		U11681
Neuronal death protein	2.3	0.0484			D83697
Poly(ADP-ribose) polymerase	1.6	0.0077			U94340
Others					
Taipoxin-associated calcium binding protein-49 precursor	−1.2	0.0032	0.0119		U15734
Cytosolic resiniferatoxin binding protein RBP-26	−1.3	0.0289	0.0358		X67877
RNA binding protein (transformer-2-like)	1.2	0.0110	0.0181		D49708
C15	−1.2	0.0002		0.0006	X82445
resection-induced TPI (rs11)	1.4	0.0011			AF007890
Anti-proliferative factor (BTG1)	−1.4	0.0484			L26268
Unknown					
EST	1.5	0.0158	0.0474	0.0026	AA892280
EST	1.2	0.0484	0.0026		AI230632
EST	1.4	0.0484		0.0078	AA894234
EST	1.2	0.0484		0.0181	AF069782

[a]The fold change was calculated between mean values of control (n = 6) and LH-S rats (n = 6). Positive values indicate an increase, and negative a decrease in gene expression in the LH.
[b]Statistical comparison was made by Mann-Whitney test (two-tailed). Only significant P-values (< 0.05) are denoted.

Activation of serotonin 2 receptors reportedly diminished γ-amino butyric acid type A receptor current through PKC in prefrontal cortical neurons.[34] Expression changes in the *Htr2a* and PKCϵ genes in LH may indicate a functional link between the two systems in the depressive state. The precise role of neurexophilin 4 in the intercellular signaling system remains unclear,[35,36] but the gene may underlie a depres-

sion/stress-related physiological pathway that cannot be corrected using TCAs or SSRIs (Table 1).

Of the LH-associated genes identified from the FC, LIMK-1 (LIM domain kinase 1: *Limk1*) displayed the most dramatic decrease, a 9.5-fold reduction compared with control levels (Table 1). Transcriptional levels were not completely normalized by imipramine or fluoxetine treatment. This

Table 2 LH-associated transcripts in the hippocampus

Functional Groups	Fold change[a]	P-value[b]			Accession No.
		Cont vs LH-S	LH-S vs LH-F	LH-S vs LH-I	
Receptor					
HGL-SL1 olfactory receptor pseudogene	−2.0	0.0005	0.0358		AF091574
olfactory receptor-like protein (SCR D-9)	−1.4	0.0050			AF034899
heparin-binding fibroblast growth factor receptor 2	−2.4	0.0373			L19112
HFV-FD1 olfactory receptor	−2.5	0.0019			AF091575
Ion channel/Transporter					
Dri 27/ZnT4 protein (zinc transporter)	1.2	0.0464	0.0181		Y16774
Chloride channel RCL1	−1.1	0.0373	0.0181		D13985
High-Affinity L-proline transporter	−1.3	0.0050		0.0078	M88111
Plasma membrane CA2+-ATPase isoform 3	−1.4	0.0018			M96626
Signal transduction					
Paranodin	1.2	0.0213	0.0078		AF000114
Arl5 (ADP-ribosylation factor-like 5)	1.4	0.0213			AA956958
Grb14	−1.4	0.0213			AF076619
Neurotransmission					
Synuclein SYN1	−1.2	0.0213	0.0358		S73007
Alpha-soluble NSF attachment protein	−1.1	0.0213		0.0078	X89968
Rab13	−1.9	0.0005		0.0358	M83678
Rab3b	−1.6	0.0213			AA799389
GTP-binding protein (ral B)	−2.0	0.0110			L19699
Neural growth/ structure					
Tuba1 (Alpha-tubulin)	1.2	0.0213	0.0006		AA892548
Zinc-finger protein AT-BP2	−1.4	0.0213			X54250
CRP2 (cysteine-rich protein 2)	−1.4	0.0373			D17512
Nfyb CCAAT binding transcription factor of CBF-B/NFY-B	−1.4	0.0373			AA817843
Decorin	−2.2	0.0213			AI639233
Metabolic enzymes					
NADH-cytochrome b-5 reductase	−1.1	0.0110	0.0358	0.0181	AI229440
Siat5 (Sialyltransferase 5)	−1.7	0.0050	0.0078		X76988
24-kDa mitochondrial NADH dehydrogenase precursor	−1.4	0.0373			M22756
2-oxoglutarate carrier	−1.4	0.0110			U84727
Soluble cytochrome b5	−1.5	0.0110			AF007107
Stress response					
Ischemia responsive 94 kDa protein (irp94)	−1.4	0.0050			AF077354
MHC class I antigen	−1.5	0.0373			AF074609
Others					
RNA splicing-related protein	−1.4	0.0373			AI044739
Aes Amino-terminal enhancer of split	−1.4	0.0153			AA875427
Proteasome RN3 subunit	−1.5	0.0110			L17127
Unknown					
EST	1.5	0.0274	0.0358		AA799488
EST	1.4	0.0373	0.0078		AA858617
EST	1.2	0.0213	0.0026		AA892817
EST	1.2	0.0050	0.0026		AA892238
EST	1.1	0.0213	0.0026		AA799893
EST	1.1	0.0050	0.0006		AA799784
EST	1.5	0.0213	0.0358		AA799525
EST	1.3	0.0373		0.0078	AA893039
EST	−1.1	0.0373		0.0358	AI007820
EST	−1.3	0.0373		0.0358	AA875348
EST	2.4	0.0213			AA875633
EST	1.9	0.0373			AI229655
EST	1.5	0.0373			AA955477
EST	1.5	0.0213			AA893569
EST	1.4	0.0464			AA800803
EST	−1.6	0.0274			AI639477
EST	−1.6	0.0110			AA892353

[a]The fold change was calculated between mean values of control ($n = 6$) and LH-S rats ($n = 6$). Positive values indicate an increase, and negative values (in red) a decrease in gene expression in the LH.

[b]Statistical comparsion was made by Mann-Whitney test (two-tailed). Only significant P-values (< 0.05) are denoted.

Table 3 Gene expression levels evaluated by quantitative RT-PCR and comparisons with the results from microarray analysis

	Frontal cortex				Hippocampus			
	LIMK-1	HTR2A	PGDS	IP3R	SNAP	SYN1	bFGFR2	Ca^{2+}-ATPase
Control	1.00±0.42	1.00±0.57	1.00±0.19	1.00±0.48	1.00±0.36	1.00±0.44	1.00±0.21	1.00±0.31
LH-S	0.49±0.07	0.36±0.06	1.64±0.25[a]	0.97±0.20	0.61±0.14	0.54±0.17	0.88±0.23	0.80±0.37
LH-F	0.50±0.06	0.57±0.26	1.10±0.20	0.52±0.15	0.86±0.14	0.65±0.23	0.65±0.11	0.80±0.14
LH-I	0.44±0.08	0.53±0.08[b]	0.81±0.33	0.72±0.23	1.45±0.51	0.30±0.07	0.52±0.16	0.70±0.29
Fold change evaluated by RT-PCT (Cont vs LH-S)	−2.0	−2.8	1.6	−1.0	−1.6	−1.9	−1.1	−1.3
Fold change evaluated by microarray (Cont vs LH-S)	−9.5	−1.6	1.3	−1.1	−1.1	−1.2	−2.4	−1.4

The expression level of each gene is normalized to that of the GAPDH gene (mean±SE, $n=6$, each in control and LH-S, $n=5$, each in LH-F and LH-I). The gene abbreviations are: LIMK-1, LIM domain kinase 1; HTR2A, 5-hydroxytryptamine (serotonin) receptor 2A; PGDS, prostaglandin D synthetase; IP3R, inositol-1,4,5-triphosphate receptor type 1; SNAP, synaptosomal-associated protein; SYN1, synuclein 1; bFGFR2, heparin-binding fibroblast growth factor receptor 2; Ca^{2+}-ATPase, plasma membrane Ca^{2+}-ATPase isoform 3.
[a]$P<0.05$ (control vs LH-S).
[b]$P<0.05$ (LH-S vs LH-I) by Mann–Whitney test (two-tailed).

partial recovery might be due to the low level of normal transcription and the large variation of expression values (supplementary Table S3). We therefore performed real-time RT-PCR to confirm the expression profile of Limk1, and detected a two-fold decrease in LH compared to control animals. This reduction was not recovered by antidepressant treatments (Table 3). Limk1 is expressed in both fetal and adult nervous systems, and shows ubiquitous expression in the brain with the strongest expression in adult cerebral cortex.[37] Recently, Limk1-knockout mice were reported to show abnormalities in spine morphology and enhanced long-term potentiation, accompanied by alterations in fear response and spatial learning.[38] A test of depression-related behavioral parameters in these mice would be intriguing. Additional reports that depressive patients frequently manifest subcortical hyperintensity near frontal white matter ('myelin pallor' on histological examination)[39] suggest that LIMK1 may be involved in an as yet undetermined intercellular signaling pathway disrupted in depression, as LIMK1 is known to phosphorylate myelin basic proteins.[40]

Our criteria for selecting 'altered' transcripts in LH compared to control animals may have been conservative and inadvertently excluded many potential candidates. Decreased levels of brain-derived neurotrophic factor (BDNF) recoverable by antidepressant treatment have been reported in patients with depression.[41,42] Although we could not detect any significant difference in expression between control and LH-S animals, we found that expression of BDNF in the FC was increased in LH-I animals compared with LH-S and control animals (supplementary Table S3).

LH-associated Transcripts Specific to the HPC and Common to Both the FC and HPC
In contrast to the FC, most LH-associated genes in the HPC showed decreased expressions on the induction of LH (Table 2). Genes coding for receptors were downregulated in both regions, although there was no overlap between the two

groups of receptors. This category included three olfactory receptor-like genes, HGL-SL1 olfactory pseudogene, olfactory receptor-like protein (SCRD-9) and HFV-FD1 olfactory receptor. Although these are thought to encode G protein-coupled receptors with seven transmembrane domains, the biological functions are unclear. Heparin-binding fibroblast growth factor receptor 2 (Fgfr2) genes were also downregulated in LH-S, but were unaffected by antidepressants (Table 2). We also found a reduction in the N-methyl-D-aspartate receptor 2A (NMDAR 2A) subunit gene in three of six LH-S animals. Fgfr2 reduces NMDAR 2A subunit mRNA levels via a receptor-mediated mechanism.[43] Chronic administration of antidepressants decreases the expression of NMDA receptor subunit genes and radioligand binding to the receptor.[42] This discrepancy warrants further investigation, to determine the role of this growth factor and the NMDA receptor genes in depression. All the LH-associated genes defined as involved in neurotransmission were also downregulated in this study (Table 2). The hippocampus is well known as a region of the brain that is highly susceptible to stress.[44,45] Recent studies have demonstrated that repeated stress causes shortening and debranching of dendrites in the CA3 region of the HPC and suppresses neurogenesis of granule neurons in the dentate gyrus.[45,46] In addition, chronic antidepressant treatment increases cell populations and neurogenesis in the rat hippocampus.[15] The extensive suppression of gene expression observed in our LH model may be related to phenotypic changes in the hippocampus produced by stress.

An unexpected finding was the scarcity of common transcripts between the two areas of brain. Of the LH-associated genes, only those coding for the 24-kDa mitochondrial NADH dehydrogenase and Dri27/ZnT4 (zinc transporter) were common to both the FC and HPC (Tables 1 and 2). However, the direction of change differed between the two regions. This selectivity was also seen in genes that were not affected by LH, but displayed a response to

Table 4 List of genes contributing to the first component in principal component analysis

Brain region[a]	Eigenvalue	Gene name[b]	Function[c]	Fold change	Accession no	Locus[d]
Frontal cortex	0.2197	Rapamycin and FKBP12 target-1 protein (rRAFT)	Stress response	1.1	U11681	5q36
	0.2194	F1-ATPase epsilon subunit	Metabolic enzyme	1.1	AI171844	20q13.3
	0.1965	Jagged2 precursor		1.3	U70050	14q32
	0.1929	24-kDa subunit of mitochondrial NADH dehydrog	Metabolic enzyme	1.4	M22756	18p11.31-p11.2
	0.1876	Bleomycin hydrolase	Metabolic enzyme	1.4	D87336	17q11.2
	0.1820	EST	Unknown	1.4	AA894234	—
	0.1760	Poly(ADP-ribose) polymerase	Stress response	1.6	U94340	1q41-q42
	0.1617	EST	Unknown	1.2	AI230632	—
	0.1531	Resection-induced TPI (rs11)	Others	1.4	AF007890	12p13
	0.1525	EST	Unknown	1.2	AF069782	—
Hippocampus	0.2114	HGL-SL1 olfactory receptor pseudogene		-2.0	AF091574	—
	0.2092	Proteasome RN3 subunit	Others	-1.5	L17127	1q21
	0.2019	24-kDa mitochondrial NADH dehydrogenase prec	Metabolic enzyme	-1.4	M22756	18p11.31-p11.2*
	0.1997	HFV-FD1 olfactory receptor		-2.5	AF091575	—
	0.1983	Soluble cytochrome b5	Metabolic enzyme	-1.5	AF007107	18q23*
	0.1865	2-Oxoglutarate carrier	Metabolic enzyme	-1.4	U84727	17p13.3
	0.1845	Grb14	Signal transduction	-1.4	AF076619	2q22-q24
	0.1626	EST	Unknown	-1.6	AA892353	—
	0.1606	GTP-binding protein (ral B)	Signal transduction	-2.0	L19699	2cen-q13
	0.1595	Rab3b	Signal transduction	-1.6	AA799389	1p32-p31*

[a]The 10 largest contributing genes to the first component in each region are listed.
[b]The genes in black indicate those up-regulated in LH animals compared to controls, while genes in red are down-regulated.
[c]The gene functions are color coded according to functional properties.
[d]*indicates that the chromosomal region shows genetic linkage to bipolar disorder.

treatment with fluoxetine, imipramine or both. In this case, from the three subsets (green, light blue and purple areas in Figure 4), five of 105 transcripts were common to both the FC and HPC (supplementary Tables S3 and S4). These findings may highlight region-specific molecular mechanisms involved in the etiology of LH. In human studies, decreased mitochondrial function was demonstrated in the basal ganglia of chronic schizophrenics,[47,48] and inhibition of mitochondrial respiratory complex I activity was reported as a cellular pathology of Parkinson's disease.[49,50] Evidence, including that of decreased ATP in frontal lobes detected in depressive patients,[51] has generated speculation about the role of mitochondrial dysfunction in depression.[52,53] NADH dehydrogenase is located on human chromosome 18 at p11.31–p11.2, a susceptibility region for affective disorder and schizophrenia.[3,54,55] These data suggest a possible link between mitochondrial NADH dehydrogenase and neuropsychiatric illnesses, including depression. The observed alteration in levels of a zinc transporter gene may tie in with recent reports that zinc exerts an antidepressant-like effect in the rodent forced swimming test,[56] and that patients with major depression demonstrate lower serum zinc levels.[57] This may imply perturbed zinc metabolism in depression, but the precise mechanisms are poorly understood.

Given that imipramine was more effective in improving LH behavior than fluoxetine, it may seem contradictory that a larger number of LH-associated transcripts showed a greater response to fluoxetine than to imipramine (Figure 4). Imipramine-responsive transcripts are likely to play a more pivotal role in behavioral recovery.

We also applied parametric statistical analysis (Student's *t*-test) to our array data. The total number of transcripts detected was slightly lower in both the FC and HPC compared to numbers detected by nonparametric tests (3 and 12 fewer in the FC and HPC, respectively). Between the two statistical methods, 10 genes in the FC (32%) and three genes in the HPC (8%) were different (supplementary Tables S7 and S8).

PCA on Altered Transcripts

PCA is a mathematical technique that exploits essential factors to define patterns in data, reducing the effective dimensionality of gene-expression space without significant loss of information.[58] This technique can be applied to both genes and experiments as a means of classification. When genes are variables, the analysis creates a set of principal gene components highlighting features of genes that best explain their experimental responses. We used the LH-associated transcripts from the FC and HPC separately as variables in PCA, to allow for better visualization of the region-specific data sets. Figures 5a and b indicate the eigenvalue distributions on the components in the FC and HPC samples, respectively. The sudden drop in eigenvalues with increasing component number suggests that it is possible to select a small number of components modeling the gene-expression differences among rat groups. We chose a three-component model for both the FC and HPC, which
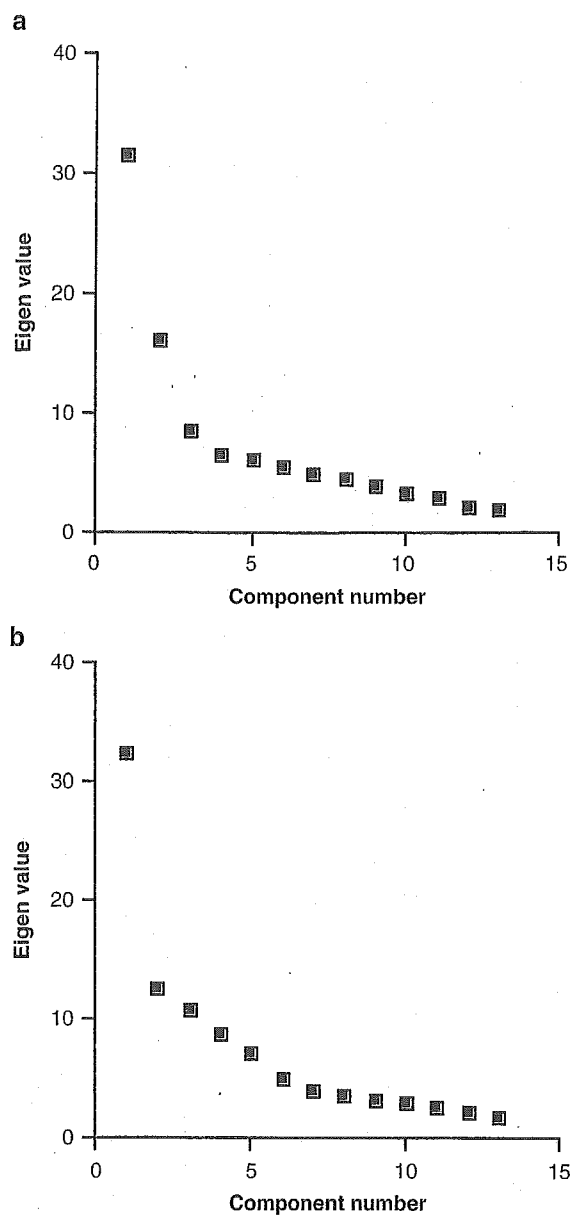

Figure 5 Component number *vs* eigenvalue in the FC (a) and the HPC (b).

explained 56% of the total variability seen in the 34 transcripts from the FC and the 48 transcripts from the HPC. The extracted dimensions represent the linear organization of data from independent systems. Each animal was plotted in a three-dimensional subspace (Figures 6a and b). The first components retain the maximal amount of correlated information (ie coordinated activity of genes) restricting the uncorrelated information to higher order components. In the FC, the first component (axis) showed good separation for the four experimental groups (control, LH-S, LH-F and LH-I), placing the antidepressant-treated groups between the control and LH-S groups. Table 4 shows
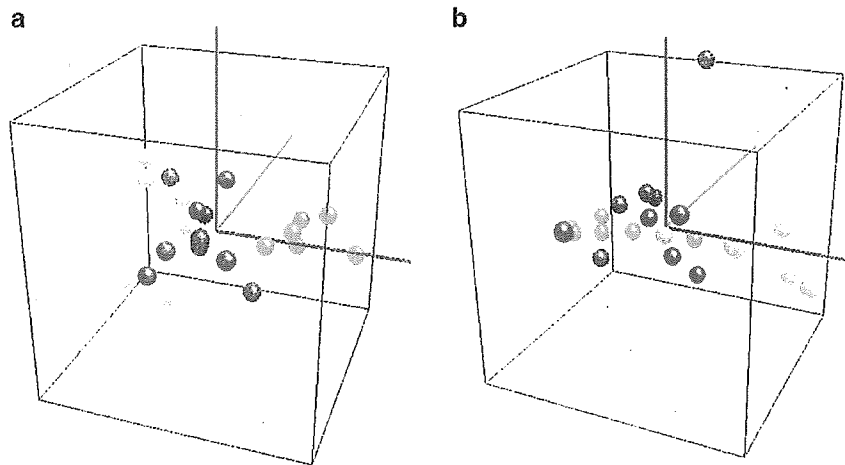
Figure 6 All animals were plotted with respect to the first (blue), second (green) and third (red) principal components. PCA was performed on transcripts listed in Table 1 (frontal cortex) (a) and Table 2 (hippocampus) (b). Yellow-colored dots represent control animals, green LH-S rats, red LH-F and blue LH-I.

transcripts from the FC that were arranged according to the magnitude of correlation with the first component (PC1) (those to the second and third components are shown in supplementary Table S5). They comprised genes for metabolic enzymes and stress responses. All genes listed in PC1 were increased in LH animals compared to controls. Among the genes coding for metabolic enzymes, the F1-ATPase epsilon subunit and 24-kDa subunit of mitochondrial NADH dehydrogenase are both localized to the mitochondria, further suggesting an important role for mitochondrial function in depression.[53] The second and third components in the FC did not further subdivide the experimental groups (supplementary figure S1). However, based on the data including the second component of PCA in the FC (supplementary Table S5), we speculate that genes responsible for neuronal growth and structure including Limk1 could be key factors in depression/stress-related pathology. In downstream pathways, alterations of these genes may affect recruitment and maintenance of multiple neurotransmitter receptors.[38] In support of this theory, structural abnormalities have recently been reported in the frontal lobe white matter of depressive patients.[59]

According to PC1 in the HPC, LH-S rats were separated from controls, with the drug-treated animals being more closely localized than the LH-S group (Figure 6b). This highlights the limited efficacy of TCA and SSRI antidepressants against dysregulated genes in the HPC, although these drugs reversed the behavioral phenotype of LH rats. The genes contributing to PC1 from the HPC would therefore represent suitable targets for future novel antidepressants. PC1 in the HPC contained genes that were downregulated in LH rats and were clustered as metabolic enzyme and signal transduction (Table 4). The second component in the HPC detected eight genes that correlated with responsiveness to fluoxetine (supplementary Table S6 and Figure S2). One

animal was separated from the others along the third component (Figure 6b). The reason for this was not clear. The animal may have suffered from highly aberrant expression of metabolic enzyme- and signal transduction-related genes and other transcripts (Table 4). Finally, the fact that the 24-kDa subunit of mitochondrial NADH dehydrogenase was extracted from both the FC and HPC with high eigenvalues is intriguing, suggesting that this gene may represent an indicator of depressive state. Moreover, the two genes, for soluble cytochrome b5 on 18q23 and Rab3 on 1p32-p31, mapped to reported linkage regions for bipolar disorder.[60]

MATERIALS AND METHODS
Animals and Experimental Design
Male Sprague–Dawley rats, 5–6-week old, weighing 150–180 g, were purchased from SLC (Shizuoka, Japan). They were housed three per cage under standard laboratory conditions, with access to food and water ad libitum. After 1 week of handling, the animals were used for experiments. Antidepressants, imipramine and fluoxetine were purchased from SIGMA (St Louis, MO, USA).

On day 1, animals were subjected to IS pretreatment (0.5 mA, 10 s duration, shock interval 1–5 s, 160 trials) in a Plexiglas chamber ($460 W \times 200 D \times 180 H$ mm^3, Muromachi, Tokyo, Japan). Two rats were processed simultaneously using two chambers. Control rats were placed for 1 h in the same chambers, but no shocks were administered.

On day 2, to evaluate escape and avoidance performance, avoidance training was initiated 24 h after IS pretreatment in the same chamber, which had been converted to a two-way shuttle box by dividing it into two equal-sized compartments using an aluminum partition. The partition included a square gate (6 × 6 cm^2), through which animals

could move into the adjacent compartment. Animals were subjected to 15 avoidance trials with 30 s intervals. In each trial, 0.5 mA of current was applied via the grid floor during the first 3 s. If an animal crossed the gate and moved to the other compartment within this period (escape response), the shock was terminated. Failures in escape response were counted as a measure of LH. Animals were defined as suffering from LH when they showed eight or more failures during a session. Control rats and a proportion of LH rats (LH-S) were administered saline once a day for three consecutive days, starting on day 2 after the avoidance trial. The remaining LH animals were treated using either imipramine (25 mg/kg, i.p.) (LH-I) or fluoxetine (5 mg/kg, i.p.) (LH-F).

On day 5, 30 min after the final injection, rats were tested for escape ability under escapable shock conditions. Among LH-I and LH-F rats, only those animals that showed a > 50% successful escape response (ie < 8 failures in the 15 trials; all LH-I rats fulfilled this criterion) were used for gene-expression analysis.

The present protocol was approved by the RIKEN animal committee.

RNA Preparation and Array Hybridization

Animals were killed on day 6, 24 h after the final electro-shock procedure. Total RNA was extracted from the FC (defined as the region anterior to the genu of corpus callosum, with the ventral olfactory structures depleted) and HPC using an acid guanidium thiocyanate/phenol chloroform extraction method (ISOGEN, NIPPON Gene, Toyama, Japan). Double-stranded cDNA was synthesized from 10 μg of total RNA using the SuperScript Choice System (Invitrogen, Carlsbad, CA, USA) and a primer containing poly (dT) and a T7 RNA polymerase promoter sequences (Geneset, La Jolla, CA, USA). Biotin-labeled cRNA was synthesized from cDNA using an Enzo BioArray High Yield RNA Transcript Labeling kit (Enzo Diagnostics, Santa Clara, CA, USA). After fragmentation, 15 μg of cRNA was hybridized for 16 h at 45°C to a U34A chip (Affymetrix, Santa Clara, CA, USA) that contained probes for over 8000 transcripts, including all known rat genes (http://www.affymetrix.com/products/netaffx.html). After hybridization, arrays were washed automatically and stained with streptavidin–phycoerythrin using the fluidics system. Chips were scanned using a GeneArray scanner (Affymetrix).

Data Analysis

All samples were scaled to a target intensity of 100. Data analysis was performed using Microarray Suite 4.0 (Affymetrix) and GeneSpring 4.1 (Silicon Genetics, Redwood, CA, USA). Transcripts with an 'average difference' (as described in the GeneChip software) of < 20 for each probe set in controls were excluded (5157 genes were selected out of 8799). From the remaining transcripts, those that gave an 'absolute call' of 'P' (present) for at least four samples in six for control and LH-S rats were considered for further analysis (3541 genes were chosen).

Before statistical analysis, each transcript was converted into a logarithmic value and normalized to itself by making a synthetic positive control and dividing all measurements by this control, assuming that the control value was at least 0.01. A synthetic control is the median of the transcript's expression values over all the samples. Two-group comparison was conducted for each transcript by a Mann–Whitney test between: (i) control and LH-S groups, (ii) LH-S and LH-F groups and (iii) LH-S and LH-I groups. The results are illustrated as a Venn diagram (Figure 2), where the overlapping areas representing (i)-, (ii)- and (iii)-type comparisons include transcripts that were selected solely using Mann–Whitney test ($P < 0.05$) and Student's t-test ($P < 0.05$). Transcripts in non-overlapping areas represent genes whose expressional changes between the two states displayed $\geqslant 1.4$-fold difference, in addition to fulfilling the P-value criteria. We also evaluated these selected transcripts by implementing the Benjamin and Hochbery False Discovery Rate program included in the GeneSpring software package. The differential gene expressions revealed by the microarray chips were examined using real-time quantitative reverse transcription (RT)-PCR, with a LightCycler and RNA Amplification kit SYBR Green I (Roche, Basel, Swizerland).

Principal Component Analysis

PCA is a statistical method for determining the coordinate transformation that explains the maximum amount of variance for the data.[25] PCA finds the principal components and each component is mutually orthogonal. To calculate the transformation, data were first normalized with reference to each gene, and then sample mean and sample variance–covariance matrix S were calculated from estimates of the mean and variance–covariance matrix. From this symmetrical matrix S, an orthogonal basis was calculated by determining eigenvalues and eigenvectors according to the equation:

$$|S - \lambda_i E| = 0 \qquad (1)$$

where E is an identity matrix and λ_i is the ith eigenvalue. i takes the value (1 to n), and n is the total number of genes.

$$SA_i = \lambda_i A_i \qquad (2)$$

where A_i is the ith eigenvector (n-dimension). The first and ith principal components were calculated as follows: $PC1 = \sum A_1 D$, $PCi = \sum A_i D$, where A_1 is the eigenvector with maximum eigenvalue, and D is the n-dimensional data vector. The proportion of the ith component was the ith eigenvalue divided by the total sum of all eigenvalues. Animals were projected into the first three-dimensional component space.[62,63]

CONCLUSION

In an effort to better understand the molecular and genetic bases underlying the pathophysiology of depressive disorder and to improve the rationale for the design of antidepressant drugs, we have performed DNA microarray analysis using an animal model of depression. Using Affymetrix GeneChip arrays, we have screened over 8000 rat genes and

ESTs, and identified 82 distinct transcripts (Tables 1 and 2, and supplementary Tables S1 and S2) in the FC and HPC that are relevant to LH and responsive to conventional antidepressants. To date, the strategy for designing antidepressive drugs is based on the serendipitous paradigm that the augmentation of monoaminergic activity in the central nervous system leads to therapeutic benefits.[1] However, currently available drugs have several drawbacks in terms of slow onset of action and intractable disease presents in approximately one-third of all depressive patients.[61] Given the genetically complex nature of human depression, we recognize that the present study can explain only limited aspects of depression pathology. Nevertheless, we believe that this study could give rise to new ideas for probing into the genetic mechanisms of human affective disorder and for refining the development of advanced therapeutics.

DUALITY OF INTEREST

None declared

ABBREVIATIONS

BDNF	brain-derived neurotrophic factor
EST	expressed sequence tag
FC	frontal cortex
HPC	hippocampus
IS	inescapable shocks
LH	learned helplessness
LH-F	LH rats treated with fluoxetine
LH-I	LH rats treated with imipramine
LH-S	LH rats treated with saline
NMDA	N-methyl-D-aspartate
NREM	nonrapid eye movement
PKC	protein kinase C
RT	reverse transcription
SSRI	selective serotonin reuptake inhibitor
TCA	tricyclic antidepressant

SUPPLEMENTARY INFORMATION

Supplementary Information accompanies the paper on the TPJ website (http://www.nature.com/tpj).

REFERENCES

1 Nestler EJ, Barrot M, DiLeone RJ, Eisch AJ, Gold SJ, Monteggia LM. Neurobiology of depression. Neuron 2002; 34: 13–25.
2 Fava M, Kendler KS. Major depressive disorder. Neuron 2000; 28: 335–341.
3 Detera-Wadleigh SD, Badner JA, Berrettini WH, Yoshikawa T, Goldin LR, Turner G et al. A high-density genome scan detects evidence for a bipolar-disorder susceptibility locus on 13q32 and other potential loci on 1q32 and 18p11.2. Proc Natl Acad Sci USA 1999; 96: 5604–5609.
4 Overmier JB, Seligman ME. Effects of inescapable shock upon subsequent escape and avoidance responding. J Comp Physiol Psychol 1967; 63: 28–33.
5 Telner JI, Singhal RL. Psychiatric progress. The learned helplessness model of depression. J Psychiatr Res 1984; 18: 207–215.
6 Geoffroy M, Scheel-Kruger J, Christensen AV. Effect of imipramine in the 'learned helplessness' model of depression in rats is not mimicked by combinations of specific reuptake inhibitors and scopolamine. Psychopharmacology 1990; 101: 371–375.
7 Nankai M, Yamada S, Muneoka K, Toru M. Increased 5-HT2 receptor-mediated behavior 11 days after shock in learned helplessness rats. Eur J Pharmacol 1995; 281: 123–130.
8 Willner P. A Psychobiological Synthesis. In: Depression. John Wiley & Sons: New York 1985.
9 Ferguson SM, Brodkin JD, Lloyd GK, Menzaghi F. Antidepressant-like effects of the subtype-selective nicotinic acetylcholine receptor agonist, SIB-1508Y, in the learned helplessness rat model of depression. Psychopharmacology 2000; 152: 295–303.
10 Sherman AD, Petty F. Learned helplessness decreases [^{3}H]imipramine binding in rat cortex. J Affect Disord 1984; 6: 25–32.
11 Mac Sweeney CP, Lesourd M, Gandon JM. Antidepressant-like effects of alnespirone (S 20499) in the learned helplessness test in rats. Eur J Pharmacol 1998; 345: 133–137.
12 Musty RE, Jordan MP, Lenox RH. Criterion for learned helplessness in the rat: a redefinition. Pharmacol Biochem Behav 1990; 36: 739–744.
13 Drevets WC, Price JL, Simpson Jr JR, Todd RD, Reich T, Vannier M et al. Subgenual prefrontal cortex abnormalities in mood disorders. Nature 1997; 386: 824–827.
14 Jacobs BL, Praag H, Gage FH. Adult brain neurogenesis and psychiatry: a novel theory of depression. Mol Psychiatry 2000; 5: 262–269.
15 Malberg JE, Eisch AJ, Nestler EJ, Duman RS. Chronic antidepressant treatment increases neurogenesis in adult rat hippocampus. J Neurosci 2000; 20: 9104–9110.
16 Eriksson PS, Perfilieva E, Bjork-Eriksson T, Alborn AM, Nordborg C, Peterson DA et al. Neurogenesis in the adult human hippocampus. Nat Med 1998; 4: 1313–1317.
17 Martin P, Soubrie P, Simon P. The effect of monoamine oxidase inhibitors compared with classical tricyclic antidepressants on learned helplessness paradigm. Progr Neuro-Psychopharmacol Biol Psychiatry 1987; 11: 1–7.
18 Nakagawa Y, Ishima T, Ishibashi Y, Tsuji M, Takashima T. Involvement of GABAB receptor systems in action of antidepressants. II: Baclofen attenuates the effect of desipramine whereas muscimol has no effect in learned helplessness paradigm in rats. Brain Res 1996; 728: 225–230.
19 Nakagawa Y, Sasaki A, Takashima T. The GABA(B) receptor antagonist CGP36742 improves learned helplessness in rats. Eur J Pharmacol 1999; 381: 1–7.
20 Tejedor-Real P, Mico JA, Maldonado R, Roques BP, Gibert-Rahola J. Implication of endogenous opioid system in the learned helplessness model of depression. Pharmacol Biochem Behav 1995; 52: 145–152.
21 Anthony JP, Sexton TJ, Neumaier JF. Antidepressant-induced regulation of 5-HT(1b) mRNA in rat dorsal raphe nucleus reverses rapidly after drug discontinuation. J Neurosci Res 2000; 61: 82–87.
22 Bristow LJ, O'Connor D, Watts R, Duxon MS, Hutson PH. Evidence for accelerated desensitisation of 5-HT$_{2C}$ receptors following combined treatment with fluoxetine and the 5-HT$_{1A}$ receptor antagonist, WAY 100,635, in the rat. Neuropharmacology 2000; 39: 1222–1236.
23 Tordera RM, Monge A, Del Rio J, Lasheras B. Antidepressant-like activity of VN2222, a serotonin reuptake inhibitor with high affinity at 5-HT1A receptors. Eur J Pharmacol 2002; 442: 63–71.
24 Mirnics K, Middleton AF, Lewis AD, Levitt P. Analysis of complex brain disorders with gene expression microarrays: schizophrenia as a disease of the synapse. Trends Neurosci 2001; 24: 479–486.
25 Raychaudhuri S, Stuart JM, Altman RB. Principal components analysis to summarize microarray experiments: application to sporulation time series. Pacific Symp Biocomput 2000: 455–466.
26 Wurmbach E, Yuen T, Ebersole BJ, Sealfon SC. Gonadotropin-releasing hormone receptor-coupled gene network. J Biol Chem 2001; 276: 47195–47201.
27 Papolos DF, Yu YM, Rosenbaum E, Lachman HM. Modulation of learned helplessness by 5-hydroxytryptamine2A receptor antisense oligodeoxynucleotides. Psychiatr Res 1996; 63: 197–203.
28 Wu J, Kramer GL, Kram M, Steciuk M, Crawford IL, Petty F. Serotonin and learned helplessness: a regional study of 5-HT1A, 5-HT2A receptors

and the serotonin transport site in rat brain. *J Psychiatr Res* 1999; **33**: 17–22.

29 Pandey GN, Pandey SC, Dwivedi Y, Sharma RP, Janicak PG, Davis JM. Platelet serotonin-2A receptors: a potential biological marker for suicidal behavior. *Am J Psychiatry* 1995; **152**: 850–855.

30 Velbinger K, De Vry J, Jentzsch K, Eckert A, Henn F, Muller WE. Acute stress induced modifications of calcium signaling in learned helpless rats. *Pharmacopsychiatry* 2000; **33**: 132–137.

31 Aldenhoff JB, Dumais-Huber C, Fritzsche M, Sulger J, Vollmayr B. Altered Ca(2+)-homeostasis in single T-lymphocytes of depressed patients. *J Psychiatr Res* 1997; **31**: 315–322.

32 Hayaishi O. Molecular mechanisms of sleep–wake regulation: a role of prostaglandin D2. *Philos Trans R Soc London—Ser B Biol Sci* 2000; **355**: 275–280.

33 Mizoguchi A, Eguchi N, Kimura K, Kiyohara Y, Qu WM, Huang ZL *et al.* Dominant localization of prostaglandin D receptors on arachnoid trabecular cells in mouse basal forebrain and their involvement in the regulation of non-rapid eye movement sleep. *Proc Natl Acad Sci USA* 2001; **98**: 11674–11679.

34 Feng J, Cai X, Zhao J, Yan Z. Serotonin receptors modulate GABA(A) receptor channels through activation of anchored protein kinase C in prefrontal cortical neurons. *J Neurosci* 2001; **21**: 6502–6511.

35 Missler M, Hammer RE, Sudhof TC. Neurexophilin binding to alpha-neurexins. A single LNS domain functions as an independently folding ligand-binding unit. *J Biol Chem* 1998; **273**: 34716–34723.

36 Missler M, Sudhof TC. Neurexophilins form a conserved family of neuropeptide-like glycoproteins. *J Neurosci* 1998; **18**: 3630–3638.

37 Nunoue K, Ohashi K, Okano I, Mizuno K. LIMK-1 and LIMK-2, two members of a LIM motif-containing protein kinase family. *Oncogene* 1995; **11**: 701–710.

38 Sarmiere PD, Bamburg JR, Meng Y, Zhang Y, Tregoubov V, Janus C *et al.* Head, neck, and spines. A role for LIMK-1 in the hippocampus. Abnormal spine morphology and enhanced LTP in LIMK-1 knockout mice. *Neuron* 2002; **35**: 3–5.

39 Steffens DC, Krishnan KR. Structural neuroimaging and mood disorders: recent findings, implications for classification, and future directions. *Biol Psychiatry* 1998; **43**: 705–712.

40 Okano I, Hiraoka J, Otera H, Nunoue K, Ohashi K, Iwashita S *et al.* Identification and characterization of a novel family of serine/threonine kinases containing two N-terminal LIM motifs. *J Biol Chem* 1995; **270**: 31321–31330.

41 Altar CA. Neurotrophins and depression. *Trends Pharmacol Sci* 1999; **20**: 59–61.

42 Skolnick P. Antidepressants for the new millennium. *Eur J Pharmacol* 1999; **375**: 31–40.

43 Brandoli C, Sanna A, De Bernardi MA, Follesa P, Brooker G, Mocchetti I. Brain-derived neurotrophic factor and basic fibroblast growth factor downregulate NMDA receptor function in cerebellar granule cells. *J Neurosci* 1998; **18**: 7953–7961.

44 Gould E, Tanapat P. Stress and hippocampal neurogenesis. *Biol Psychiatry* 1999; **46**: 1472–1479.

45 McEwen BS. Stress and hippocampal plasticity. *Annu Rev Neurosci* 1999; **22**: 105–122.

46 McEwen BS. Effects of adverse experiences for brain structure and function. *Biol Psychiatry* 2000; **48**: 721–731.

47 Prince JA, Blennow K, Gottfries CG, Karlsson I, Oreland L. Mitochondrial function is differentially altered in the basal ganglia of chronic schizophrenics. *Neuropsychopharmacology* 1999; **21**: 372–379.

48 Maurer I, Zierz S, Moller H. Evidence for a mitochondrial oxidative phosphorylation defect in brains from patients with schizophrenia. *Schizophr Res* 2001; **48**: 125–136.

49 Jha N, Jurma O, Lalli G, Liu Y, Pettus EH, Greenamyre JT *et al.* Glutathione depletion in PC12 results in selective inhibition of mitochondrial complex I activity. Implications for Parkinson's disease. *J Biol Chem* 2000; **275**: 26096–26101.

50 Chinopoulos C, Adam-Vizi V. Mitochondria deficient in complex I activity are depolarized by hydrogen peroxide in nerve terminals: relevance to Parkinson's disease. *J Neurochem* 2001; **76**: 302–306.

51 Volz HP, Rzanny R, Riehemann S, May S, Hegewald H, Preussler B *et al.* 31P magnetic resonance spectroscopy in the frontal lobe of major depressed patients. *Eur Arch Psychiatr Clin Neurosci* 1998; **248**: 289–295.

52 Jaksch M, Lochmuller H, Schmitt F, Volpel B, Obermaier-Kusser B, Horvath R. A mutation in mt tRNALeu(UUR) causing a neuropsychiatric syndrome with depression and cataract. *Neurology* 2001; **57**: 1930–1931.

53 Kato T. The other, forgotten genome: mitochondrial DNA and mental disorders. *Mol Psychiatry* 2001; **6**: 625–633.

54 Yoshikawa T, Kikuchi M, Saito K, Watanabe A, Yamada K, Shibuya H *et al.* Evidence for association of the myo-inositol monophosphatase 2 (IMPA2) gene with schizophrenia in Japanese samples. *Mol Psychiatry* 2001; **6**: 202–210.

55 Schwab SG, Hallmayer J, Lerer B, Albus M, Borrmann M, Honig S *et al.* Support for a chromosome 18p locus conferring susceptibility to functional psychoses in families with schizophrenia, by association and linkage analysis. *Am J Hum Genet* 1998; **63**: 1139–1152.

56 Kroczka B, Branski P, Palucha A, Pilc A, Nowak G. Antidepressant-like properties of zinc in rodent forced swim test. *Brain Res Bull* 2001; **55**: 297–300.

57 Maes M, Vandoolaeghe E, Neels H, Demedts P, Wauters A, Meltzer HY *et al.* Lower serum zinc in major depression is a sensitive marker of treatment resistance and of the immune/inflammatory response in that illness. *Biol Psychiatry* 1997; **42**: 349–358.

58 Quackenbush J. Computational analysis of microarray data. *Nat Rev Genet* 2001; **2**: 418–427.

59 Steingard RJ, Renshaw PF, Hennen J, Lenox M, Cintron CB, Yuoung AD *et al.* Smaller frontal lobe white matter volumes in depressed adolescents. *Biol Psychiatry* 2002; **52**: 413–417.

60 Cowan WM, Kopnisky KL, Hyman SE. The human genome project and its impact on psychiatry. *Annu Rev Neurosci* 2002; **25**: 1–50.

61 Skolnick P, Legutko B, Li X, Bymaster FP. Current perspectives on the development of non-biogenic amine-based antidepressants. *Pharmacol Res* 2001; **43**: 411–423.

62 Crescenzi M, Giuliani A. The main biological determinants of tumor line taxonomy elucidated by a principal component analysis of microarray data. *FEBS Lett* 2001; **507**: 114–118.

63 Landgrebe J, Welzl G, Metz T, van Gaalen MM, Ropers H, Wurst W *et al.* Molecular characterization of antidepressant effects in the mouse brain using gene expression profiling. *J Psychiatr Res* 2002; **36**: 119–129.

Association of Neural Cell Adhesion Molecule 1 Gene Polymorphisms with Bipolar Affective Disorder in Japanese Individuals

Makoto Arai, Masanari Itokawa, Kazuo Yamada, Tomoko Toyota, Mayumi Arai, Seiichi Haga, Hiroshi Ujike, Ichiro Sora, Kazuhiko Ikeda, and Takeo Yoshikawa

Background: Although the pathogenesis of mood disorders remains unclear, heritable factors have been shown to be involved. Neural cell adhesion molecule 1 (NCAM1) is known to play important roles in cell migration, neurite growth, axonal guidance, and synaptic plasticity. Disturbance of these neurodevelopmental processes is proposed as one etiology for mood disorder. We therefore undertook genetic analysis of NCAM1 in mood disorders.

Methods: We determined the complete genomic organization of human NCAM1 gene by comparing complementary deoxyribonucleic acid and genomic sequences; mutation screening detected 11 polymorphisms. The genotypic, allelic, and haplotype distributions of these variants were analyzed in unrelated control individuals (n = 357) and patients with bipolar disorder (n = 151) and unipolar disorder (n = 78), all from central Japan.

Results: Three single nucleotide polymorphisms, IVS6+32T>C, IVS7+11G>C and IVS12+21C>A, displayed significant associations with bipolar disorder (for allelic associations, nominal p = .04, p = .02, and p = .004, respectively, all p > .05 after Bonferroni corrections). Furthermore, the haplotype located in a linkage disequilibrium block was strongly associated with bipolar disorder (the p value of the most significant three-marker haplotype is .005).

Conclusions: Our results suggest that genetic variations in NCAM1 or nearby genes could confer risks associated with bipolar affective disorder in Japanese individuals.

A ffective disorder is a common psychiatric disease, afflicting approximately 10% of the population worldwide. Once the disease develops, episodes tend to recur throughout life, and prophylaxis is difficult to achieve in some cases with the therapeutic agents currently available. The etiologic bases remain unknown, although twin, family, and adoption studies have provided evidence for the involvement of heritable risk factors (Cardno et al 1999; Craddock and Jones 1999; Mendlewicz and Rainer 1977; Taylor et al 2002). Positive findings from linkage analyses and case–control association studies have also been reported (Berrettini 2000, 2001, 2002; Craddock et al 2001; Kato 2001).

Neural cell adhesion molecule 1 (NCAM1) is a member of the immunoglobulin gene superfamily and is widely expressed in the central nervous system. In addition, three major protein isoforms, of 180 kd, 140 kd, and 120 kd, are well known to possess multiple neurobiological functions in the brain (Kiss and Muller 2001; Ronn et al 1998). The genomic organization has already been partially reported (Saito et al 1994). The 180-kd and 140-kd isoforms of NCAM1 are transmembrane proteins, whereas the 120-kd isoform is linked to the plasma membrane via a glycosyl phosphatidyl-inositol (GPI) lipid anchor. Glycosyl phosphatidyl-inositol is attached to the C-terminal amino acid encoded by exon 15, the exon skipped in the transmembrane forms of NCAM 140 and NCAM 180. The difference between NCAM 140 and NCAM 180 involves the use of exon 18 by the latter isoform (Ronn et al 1998). Furthermore, some alternatively spliced exons exist between exons 7 and 13 (Barton et al 1988; Gower et al 1988; Saito et al 1994; van Duijnhoven et al 1992; also see Figure 1 legend). Several lines of evidence have supported the idea that dysregulation of NCAM1 isoforms in the brain might be involved in the pathophysiology of neuropsychiatric disorders, particularly bipolar affective disorder (Vawter 2000a). Secreted exon (SEC)-NCAM1 is increased in the hippocampus of patients with bipolar disorder (Vawter et al 1999), whereas variable alternative spliced exon (VASE)-NCAM1 is increased in the prefrontal cortex and hippocampus of patients with bipolar disorder (Vawter et al 1998). Furthermore, Poltorak et al (1996) reported elevated concentrations of NCAM1 protein in the cerebrospinal fluid of patients with mood disorder.

In this study, we performed genetic analysis of *NCAM1* as a compelling candidate for involvement in mood disorders.

Methods and Materials

Subjects

Mood disorder samples comprised unrelated patients with bipolar disorder (n = 151; 66% bipolar I, 34% bipolar II) and 78 patients with unipolar disorder (n = 78). Patients with bipolar disorder comprised 80 men (mean age, 49.0 ± 11.9 years) and 71 women (mean age, 48.9 ± 12.4 years). Patients with unipolar disorder comprised 33 men (mean age, 48.1 ± 10.7 years) and 45 women (mean age, 50.7 ± 10.9 years). All patients were diagnosed according to DSM-IV criteria for mood disorder (American Psychiatric Association 1994), to give a best-estimate lifetime diagnosis with consensus from at least two experienced psychi-
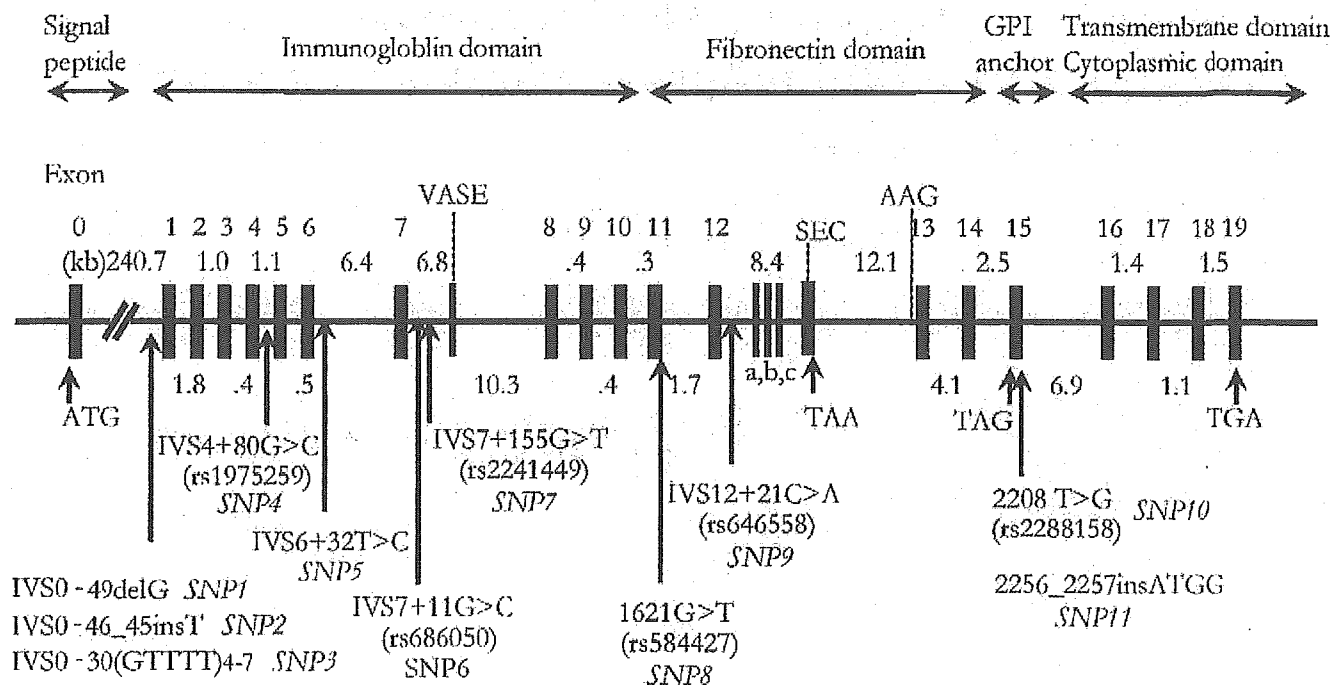
Figure 1. Genomic structure and locations of polymorphic sites for human NCAM1. Exons 0 through 14 are common in all neural cell adhesion molecule (NCAM) isoforms. In addition to the common exons, NCAM 180 uses exons 16, 17, 18, and 19; NCAM 140 uses exons 16, 17, and 19; and NCAM 120 uses exon 15. Locations of the initiation codon (ATG) and stop codons (TAA and TAG), and sizes (kilobases [kb]) of introns are provided. GPI, glycosyl phosphatidylinositol; VASE, variable alternative spliced exon; SEC, secreted exon; a, b, c, and triplet AAG, mini-exons; rs number is the National Center for Biotechnology Information single nucleotide polymorphism (SNP) cluster identification number from the dbSNP database (http://www.ncbi.nlm.nih.gov/SNP/).

atrists. The interview parameters included those described in the Structured Clinical Interview for DSM-IV Axis I Disorders (First et al 1997). All available medical records and family informant reports were also taken into consideration. Control subjects were recruited from among hospital staff and company employees documented to be free from psychoses; they included 173 men (mean age, 50.5 ± 13.5 years) and 184 women (mean age, 52.8 ± 11.0 years). All of our samples were collected from central Japan.

The present study was approved by the Ethics Committees of Tokyo Institute of Psychiatry, RIKEN Brain Science Institute, and Okayama University, and all participants provided written informed consent.

Determination of Genomic Structure

The complete genomic structure of *NCAM1* was determined by comparing complementary deoxyribonucleic acid (DNA) sequence (GenBank accession nos. NM_000615, M22094, S73101, XM_084656, X53243, and AK057509) and the University of California, Santa Cruz (UCSC) April 2003 draft assembly of the human genome (UCSC Genome Bioinformatics web site: http://genome.ucsc.edu/). We newly identified the location of exons VASE (S73101), SEC (M22094), 15 (M22094), 18 (XM_084656, AK057509), and 19 (AK057509). These sequences were not included in the UCSC's gene prediction program. "A" from the ATG initiation codon was considered +1.

Screening for Polymorphisms and Genotyping of Variants

Genomic DNA was isolated from blood samples according to standard methods. All exons and splice boundaries of *NCAM1*, except for some minor exons, were screened for polymorphisms by direct sequencing of polymerase chain reaction (PCR) prod-

ucts, from 20 unrelated bipolar samples. Primers used for PCR amplification are listed in Table 1. Polymerase chain reaction was performed with initial denaturation at 94°C for 1 min, followed by 35 cycles at 94°C for 15 sec, 50°C–70°C (optimized for each primer pair) for 30 sec, 72°C for 45 sec, and final extension at 72°C for 2 min, with TaKaRa Taq polymerase (Takara Bio, Shiga, Japan) or the Expand Long Template PCR System (Roche Diagnotics, Mannheim, Germany). Detailed information on amplification conditions is available upon request. Direct sequencing of PCR products was performed with the BigDye Terminator Cycle Sequencing FS Ready Reaction kit (Applied Biosystems, Foster City, California) and the ABI PRISM 3100 Genetic Analyzer (Applied Biosystems). All the polymorphisms were genotyped by direct sequencing with the help of the SEQUENCHER program (Gene Codes Corporation, Ann Arbor, Michigan), followed by visual inspection by two researchers. When necessary, both strands were sequenced.

Statistical Analysis

Departure from Hardy-Weinberg equilibrium was examined with the χ^2 test. Differences in genotype and allele frequencies were evaluated with Fisher's exact test or the Monte-Carlo method implemented in the CLUMP program (Sham and Curtis 1995) when appropriate. Linkage disequilibrium (LD) statistics were calculated with COCAPHASE (Dudbridge 2002; http://www.hgmp.mrc.ac.uk/~fdudbrid/software/). Estimation and comparison of haplotype frequencies were made with COCAPHASE. Graphic overview of pairwise LD strength between markers was made with GOLD software (Abecasis and Cookson 2000; http://www.well.ox.ac.uk/asthma/GOLD/). Power calculations were performed with Power Calculator (http://calculators.stat.ucla.edu/powercalc/).

Table 1. PCR Primers Used to Search for Nucleotide Variants in the *NCAM1* Gene

Region	Exon Length (bp)	Intron Length (bp)	Primers	Product Size (bp)	3' End of Primer
Exon 1	75		(F) 5'-AAACTCCACACAAACCTCCTCCC-3'	424	148 bp upstream to exon 1
		1832	(R) 5'-TGCAAAAGGAAGGAAGAGGCCC-3'		159 bp downstream to exon 1
Exon 2	219		(F) 5'-TTCCAGCAGCCATACTCACCCC-3'	498	128 bp upstream to exon 2
		1018	(R) 5'-TTAGGGAGAGAGAATGGGACTG-3'		110 bp downstream to exon 2
Exon 3	144		(F) 5'-TGGAGACTTGCCCAGGACTCA-3'	382	84 bp upstream to exon 3
		376	(R) 5'-AGGACCCAGAAACCACATGAGG-3'		113 bp downstream to exon 3
Exon 4	138		(F) 5'-TCAAAGCCAGGGACGCATTTTC-3'	429	124 bp upstream to exon 4
		1080	(R) 5'-TTACGGTGGGGAGGGGATTTA-3'		126 bp downstream to exon 4
Exon 5	118		(F) 5'-CAATTCCTGACACTAACTCTG-3'	367	124 bp upstream to exon 5
		454	(R) 5'-CCTAAGAAGCCCACATCCATT-3'		85 bp downstream to exon 5
Exon 6	170		(F) 5'-CAGTTGCAGCCCTTGGATAGT-3'	539	182 bp upstream to exon 6
		6366	(R) 5'-ATGATGGTGGCTTGGACTAGG-3'		147 bp downstream to exon 6
Exon 7	143		(F) 5'-ACTAGGGTCTTGTACTTAGCAG-3'	454	94 bp upstream to exon 7
		6784	(R) 5'-TGTGCCTATTCCATTACAAGGG-3'		175 bp downstream to exon 7
VASE	30		(F) 5'-CTAAGGGGGAAAAAAAGCTGGACA-3'	425	181 bp upstream to exon VASE
		10319	(R) 5'-TCATCCACTCCCAACACAGC-3'		173 bp downstream to exon VASE
Exon 8	151		(F) 5'-GATACTCCCAGGTTCTCATGC-3'	583	192 bp upstream to exon 8
		374	(R) 5'-ATGGGAAGAAGACTCAAGGGCA-3'		199 bp downstream to exon 8
Exon 9	185		(F) 5'-TGTTCTGCTTACGTTCCCTGCA-3'	687	256 bp upstream to exon 9
		363	(R) 5'-GAGAAAAGAATAGCAGAGGGGC-3'		204 bp downstream to exon 9
Exon 10	97		(F) 5'-TTGTTTAAGGCTGGGCTGGAG-3'	368	118 bp upstream to exon 10
		332	(R) 5'-AACTCTCTGGCTTTGCTGACC-3'		113 bp downstream to exon 10
Exon 11	171		(F) 5'-ATTGGATCAGCGCATGGGGCA-3'	508	164 bp upstream to exon 11
		1715	(R) 5'-AGGGGCAACAACTCTACAGGCA-3'		132 bp downstream to exon 11
Exon 12	132		(F) 5'-GTCATTTGGGTCTGCCTTTCGG-3'	553	215 bp upstream to exon 12
		8387	(R) 5'-GAAGGGACTGTGTGTTAGCTGTCA-3'		162 bp downstream to exon 12
SEC	239		(F) 5'-GAGGGTGATGCCGAGAAGGAA-3'	661	240 bp upstream to exon SEC
		12086	(R) 5'-CACACGGAGGGAACACCAAGA-3'		142 bp downstream to exon SEC
Exon 13	125		(F) 5'-CTCTCAGTTTGGGCTCAGTC-3'	488	168 bp upstream to exon 13
		4144	(R) 5'-GCTGTAGGGCTGTCTTGGGATT-3'		153 bp downstream to exon 13
Exon 14	178		(F) 5'-GTCCCGTAAGTTTTGCCTATTGTC-3'	434	72 bp upstream to exon 14
		2522	(R) 5'-GCACAGATAGGTACAAGGCAAAAC-3'		138 bp downstream to exon 14
Exon 15	448		(F) 5'-ACCTTCCCTTTCCTTCTGTCCC-3'	746	123 bp upstream to exon 15
		6894	(R) 5'-ATCAGTGCGGTCTGGCTCTTTTAAC-3'		130 bp downstream to exon 15
Exon 16	208		(F) 5'-CTGTTTTCTCAATTCTGGGGCATA-3'	500	148 bp upstream to exon 16
		1364	(R) 5'-CAAATGGAGAACGTGCAATGAAAG-3'		98 bp downstream to exon 16
Exon 17	117		(F) 5'-AAGCTCAAGGTCACACAGCTAG-3'	680	147 bp upstream to exon 17
		1056	(R) 5'-GGTCCCCAGCTTCCCTTATCCTTT-3'		372 bp downstream to exon 17
Exon 18	816		(F) 5'-ATCCTTCTCTCTCTGTGGGCCT-3'	1055	133 bp upstream to exon 18
		1518	(R) 5'-CATCTAACAAGGAGGACACAGCAC-3'		62 bp downstream to exon 18
Exon 19	298		(F) 5'-CTTGGGTGATTTTTAGTGCTCC-3'	1071	146 bp upstream to exon 19
			(R) 5'-GGCAGCTATTTTACACGGACAT-3'		585 bp downstream to exon 19

PCR, polymerase chain reaction; NCAM1, neural cell adhesion molecule 1; F, forward; R, reverse; VASE, variable alternative spliced exon; SEC, secreted exon.

Results

The complete human *NCAM1* spans a region of 314 kilobases (kb) on chromosome 11q23.1, and consists of 19 main exons, exon 0 that encodes the signal peptide, alternatively spliced VASE and SEC exons, and the three-base-pair mini-exon AAG (Figure 1). Two or more alternatively spliced small exons (exons a, b, and c in Figure 1) exist between exons 12 and 13. Although protein isoforms are detected as three major mass classes (180, 140, and 120 kd), combinations of these exons and posttranslational modifications give rise to 20–30 molecular species for NCAM1 (Goridis and Brunet 1992; Kiss and Muller 2001).

Mutation screening allowed us to identify 11 polymorphisms, including five novel variants: IVS0–49delG, IVS0–46_45insT, IVS0–30(GTTTT)$_{4-5}$, IVS6+32T>C, and 2256_2257insATGG

(Figure 1). For brevity, the detected single nucleotide polymorphisms (SNPs) were designated as SNP1–11 (Figure 1; Tables 2 and 3). The frequencies (except for that of IVS0–46_45insT, SNP2) are summarized in Tables 2 (SNP3) and 3 (SNPs 1, 4–11). The IVS0–46_45insT genotype could not be accurately determined, owing to the homopolymeric stretch of T nucleotides [(T)$_9$ or (T)$_{10}$]. This polymorphism was thus excluded from subsequent analyses. All polymorphisms were in Hardy-Weinberg equilibrium. Of the 10 polymorphisms, IVS12+21C>A (NCBI dbSNP accession no. rs646558, http://www.ncbi.nlm.nih.gov/SNP/) displayed a nominally significantly different genotypic distribution between patients with bipolar disorder and control subjects ($p = .01$; Table 3). IVS6+32T>C (novel) and IVS7+11G>C (rs686050) displayed trends toward genotypic association with bipolar disease.

www.elsevier.com/locate/biopsych

Table 2. Genotypic and Allelic Distributions of the *NCAM1* Gene Polymorphism, IVS0–30 (GTTTT)$_{4-7}$

IVS0–30(GTTTT)$_{4-7}$ (SNP3)	Bipolar Disorder ($n = 151$)	Unipolar Disorder ($n = 78$)	Control Subjects ($n = 357$)
Genotype Counts (Frequency)			
4/4	64 (.42)	25 (.32)	122 (.34)
4/5	24 (.16)	12 (.15)	68 (.19)
4/6	35 (.23)	23 (.29)	92 (.26)
4/7	10 (.07)	2 (.03)	18 (.05)
5/5	3 (.02)	1 (.01)	4 (.01)
5/6	4 (.03)	5 (.06)	18 (.05)
5/7	3 (.02)	3 (.04)	8 (.02)
6/6	4 (.03)	7 (.09)	14 (.04)
6/7	3 (.02)	0 (0)	13 (.04)
7/7	1 (.01)	0 (0)	0 (0)
p^a	.44	.36	
Allele Counts (Frequency)			
4	197 (.65)	87 (.56)	422 (.59)
5	37 (.12)	22 (.14)	102 (.14)
6	50 (.17)	42 (.27)	151 (.21)
7	18 (.06)	5 (.03)	39 (.05)
p^a	.25	.33	

NCAM1, neural cell adhesion molecule 1.
[a]Differences in genotypic and allelic distributions were evaluated by the Monte Carlo method.

Allelic distributions in the above three polymorphisms all displayed significant deviations in bipolar samples compared with control subjects: IVS6+32T>C, nominal $p = .04$, odds ratio (OR) = 1.47, 95% confidence interval (CI) = 1.03–2.10; IVS7+11G>C, nominal $p = .02$, OR = 1.37, 95% CI = 1.05–1.80; IVS12+21C>A, nominal $p = .004$, OR = 1.64, 95% CI = 1.18–2.28 (Table 3). After Bonferroni correction for multiple testing of 10 SNPs and two disease classifications, these deviations were not significant. For unipolar disorder, none of these polymorphisms displayed nominally significant genotypic or allelic associations with the disease.

Power calculations were performed on the basis of an arbitrary assumption of relative risk and frequency of risk allele. When a relative risk of 2.0 was assumed, the bipolar sample in the present study displayed ≥93% power to detect significant association ($\alpha < .05$, frequency of risk allele = .3). The unipolar samples had ≥76% power. With a relative risk of 1.5, our bipolar samples had 51% power to detect significant association ($\alpha < .05$, frequency of risk allele = .3). The unipolar samples retained 34% power.

Common (frequency of minor allele > .03) variants in the gene were selected for pairwise LD testing: IVS4+80G>C (SNP4); IVS6+32T>C (SNP5); IVS7+11G>C (SNP6); IVS7+155G>T (SNP7); 1621G>T (SNP8); IVS12+21C>A (SNP9); and 2208T>G (SNP10) (Figure 1, Table 4). IVS0–49delG (SNP1) and IVS0–30(GTTTT)$_{4-7}$ (SNP3) were also included for LD calculations to examine the 5′ upstream genomic structure of *NCAM1*. *D′* (normalized *D*) and r^2 (squared correlation coefficient) values were computed in patients with bipolar disorder and control subjects. Both LD measures take values between 0 (lack of LD) and 1 (complete LD). Abecasis et al (2001) suggested a *D′* value of >.33 as a useful measure of LD. Nakajima et al (2002) proposed $r^2 > .1$ as a criterion for useful LD. Linkage disequilibrium relationships between markers are shown graphically in Figure 2. Linkage disequilibrium structure was similar in

the two measures (also see Table 4). These data revealed that the region spanning SNP1 through SNP9 was in a block of moderate-to-strong LD, and there was an overt LD gap between SNP9 and SNP10. Polymorphisms associated with bipolar disorder displayed relatively strong LD between IVS6+32T>C (SNP5) and IVS7+11G>C (SNP6) ($D′ = 1.00$, $r^2 = .181$) and between IVS6+32T>C (SNP5) and IVS12+21C>A (SNP9) ($D′ = .728$, $r^2 = .397$), but not between IVS7+11G>C (SNP6) and IVS12+21C>A (SNP9) ($D′ = .277$, $r^2 = .019$) (Table 4).

Next, we examined three SNP-based haplotypic associations in a sliding manner in the bipolar group, with the polymorphisms that spanned the LD block (SNP1–9) (Figure 3, Table 5). All the three SNP combinations except for SNP5-6-7 and SNP6-7-8 showed significant association with bipolar disorder in terms of both global p values and p values for individual risk haplotypes. The haplotypes defined by SNP5-6-7 displayed significant individual haplotypic association ($p = .034$) and a trend of global association ($p = .097$), whereas those constructed by SNP6-7-8 showed marginal individual haplotypic association ($p = .067$) (Figure 3). These haplotype analyses demonstrated that the risk haplotype consisting of SNP1–9 for bipolar disorder was Ins-(GTTTT)$_4$-G-C-C-G-G-A (global $p = .033$, individual haplotype $p = .009$) (Figure 3, Table 5).

Discussion

Neural cell adhesion molecule 1 is essential for cell adhesion, cell migration, axonal guidance, signal transduction, and synaptic plasticity during brain development. Bouras et al (2001) reported decreased neuron densities in layers III, V, and VI of Brodmann's area 24 (anterior cingulate cortex) in patients with bipolar disorder. Densities of neurons and pyramidal and glial cells were reduced in the prefrontal cortex of bipolar patients (Rajkowaska et al 2001). Animal studies have also suggested that disruption of NCAM1 function might underlie the pathophysiology of affective disorder through dysregulation of the cytoarchitecture (Cremer et al 1994; Tomasiewicz et al 1993). *NCAM1* is therefore deemed to possess compelling functional relevance to affective disorders.

Our case–control analysis revealed that the IVS6+32T>C (SNP5), IVS7+11G>C (SNP6), and IVS12+21C>A (SNP9) polymorphisms of *NCAM1* are nominally significantly associated with bipolar disorder, with the IVS12+21A (SNP9) allele displaying the strongest association (allelic $p = .08$ after correction for 10 SNPs and two disease category examinations). Sixty-six percent of our bipolar subjects suffered from bipolar disorder type I. It might be possible that bipolar I and bipolar II disorders are separate entities; however, there seems to be no difference in genetic association with *NCAM1* between bipolar I and II groups in the present study: allele frequencies of IVS12+21A (SNP9), which showed the strongest p value, were similar in bipolar I (.23, allelic $p = .067$) and bipolar II (.26, allelic $p = .058$) cohorts. Linkage disequilibrium analysis revealed that IVS12+21C>A (SNP9) was located at the 3′ edge of the LD block, and a gap existed between SNP9 and the neighboring SNP10. These results suggest that the real disease-causing variant(s), if one exists, might reside in the 3′ portion of the haplotype block spanning SNP1 to SNP10. The association of IVS6+32T>C (SNP5) and IVS7+11G>C (SNP6) polymorphisms with bipolar disorder might reflect tapering but remnant LD between these polymorphisms and the neighboring risk variant(s); however, more thorough genetic analyses are needed to precisely locate the genomic boundaries contributing to the development of bipolar disorder.

Table 3. Genotypic and Allelic Distributions of Nine *NCAM1* Gene Polymorphisms

Polymorphism	n	Genotype Counts (Frequency)			p^a	Allele Counts (Frequency)		p^a
IVS0-49de IG (SNP1)		I/I	I/D	D/D		I	D	
Bipolar disorder	151	128 (.85)	22 (.15)	1 (.01)	.89	278 (.92)	24 (.08)	.55
Unipolar disorder	78	64 (.82)	13 (.17)	1 (.01)	.95	141 (.90)	15 (.10)	.89
Control subjects	357	295 (.83)	58 (.16)	4 (.01)		648 (.91)	66 (.09)	
IVS4 + 80G > C (SNP4)		G/G	G/C	C/C		G	C	
Bipolar disorder	151	63 (.42)	68 (.45)	20 (.13)	.17	194 (.64)	108 (.36)	.08
Unipolar disorder	78	25 (.32)	38 (.49)	15 (.19)	.85	88 (.56)	68 (.44)	.72
Control subjects	357	118 (.33)	180 (.50)	59 (.17)		416 (.58)	298 (.42)	
IVS6 + 32T > C (SNP5)		T/T	T/C	C/C		T	C	
Bipolar disorder	151	96 (.64)	51 (.34)	4 (.03)	.06	243 (.80)	59 (.20)	.04
Unipolar disorder	78	59 (.76)	17 (.22)	2 (.03)	.37	135 (.87)	21 (.13)	.90
Control subjects	357	260 (.73)	93 (.26)	4 (.01)		613 (.86)	101 (.14)	
IVS7 + 11G > C (SNP6)		G/G	G/C	C/C		G	C	
Bipolar disorder	151	25 (.17)	79 (.52)	47 (.31)	.06	129 (.43)	173 (.57)	.02
Unipolar disorder	78	25 (.32)	34 (.44)	19 (.24)	.45	84 (.54)	72 (.46)	.48
Control subjects	357	91 (.25)	179 (.50)	87 (.24)		361 (.51)	353 (0.49)	
IVS7 + 155G > T (SNP7)		G/G	G/T	T/T		G	T	
Bipolar disorder	151	127 (.84)	23 (.15)	1 (.01)	1.00	277 (.92)	25 (.08)	.90
Unipolar disorder	78	64 (.82)	13 (.17)	1 (.01)	.89	141 (.90)	15 (.10)	.76
Control subjects	357	298 (.83)	55 (.15)	4 (.01)		651 (.91)	63 (.09)	
I621G > T (SNP8)		G/G	G/T	T/T		G	T	
Bipolar disorder	151	61 (.40)	74 (.49)	16 (.11)	.64	196 (.65)	106 (.35)	.38
Unipolar disorder	78	42 (.54)	29 (.37)	7 (.09)	.28	113 (.72)	43 (.28)	.29
Control subjects	357	159 (.45)	166 (.46)	32 (.09)		484 (.68)	230 (.32)	
IVS12 + 21 C > A (SNP9)		C/C	C/A	A/A		C	A	
Bipolar disorder	151	87 (.58)	54 (.36)	10 (.07)	.01	228 (.75)	74 (.25)	.004
Unipolar disorder	78	51 (.65)	26 (.33)	1 (.01)	.51	128 (.82)	28 (.18)	.64
Control subjects	357	249 (.70)	98 (.27)	10 (.03)		596 (.83)	118 (.17)	
2208T > G (SNP10)		T/T	T/G	G/G		T	G	
Bipolar disorder	151	79 (.52)	64 (.42)	8 (.05)	.15	222 (.74)	80 (.26)	.23
Unipolar disorder	78	36 (.46)	36 (.46)	6 (.08)	.54	108 (.69)	48 (.31)	.92
Control subjects	357	178 (.50)	141 (.39)	38 (.11)		497 (.70)	217 (.30)	
2256_2257 insATGG (SNP11)		D/D	D/I	I/I		D	I	
Bipolar disorder	151	143 (.95)	8 (.05)	0 (.00)	.32	294 (.97)	8 (.03)	.33
Unipolar disorder	78	78 (1.00)	0 (.00)	0 (.00)	.14	156 (1.00)	0 (0.00)	.14
Control subjects	357	345 (.97)	12 (.03)	0 (.00)		702 (.98)	12 (.02)	

NCAM1, neural cell adhesion molecule 1; I, insertion; D, deletion; SNP, single nucleotide polymorphism.
^{a}Differences in genotypic and allelic distributions were evaluated by Fisher's exact test.

Interestingly, IVS6+32T>C, IVS7+11G>C, and IVS12+21C>A were all located in close proximity to the intron–exon boundaries. Mutations located near splicing donor and acceptor sites were found in patients with frontotemporal dementia, FTDP-17, and affected splicing regulation of τ-protein by causing distortion of the stem-loop structure (Hutton et al 1998). Previous postmortem studies have shown that the VASE- and SEC-NCAM isoforms are increased in the brains of patients with bipolar disorder,

Table 4. Pairwise Linkage Disequilibrium Estimations Between Polymorphisms in the *NCAM1* Gene

Polymorphism	IVS0-49delG (SNP1)	IVS0-30(GTTTT)$_{4-7}$ (SNP3)	IVS4 + 80 G > C (SNP4)	IVS6 + 32 T > C (SNP5)	IVS7 + 11 G > C (SNP6)	IVS7 + 155 G > T (SNP7)	1621 G > T (SNP8)	IVS12 + 21 C > A (SNP9)	2208 T > G (SNP10)
SNP1		1.000 (1.000)	1.000 (1.000)	1.000 (1.000)	1.000 (1.000)	1.000 (1.000)	1.000 (1.000)	.351 (.450)	.277 (.150)
SNP3	.070 (.046)		.944 (1.000)	1.000 (1.000)	.923 (1.000)	1.000 (1.000)	.882 (.792)	.699 (.670)	.112 (.088)
SNP4	.071 (.048)	.838 (.957)		1.000 (1.000)	.885 (.947)	1.000 (1.000)	.896 (.770)	.469 (.601)	.125 (.065)
SNP5	.017 (.021)	.112 (.129)	.114 (.131)		1.000 (1.000)	1.000 (1.000)	1.000 (1.000)	.534 (.728)	.141 (.015)
SNP6	.098 (.116)	.547 (.715)	.548 (.670)	.169 (.181)		.900 (.756)	.847 (.818)	.005 (.277)	.136 (.087)
SNP7	1.000 (1.000)	.067 (.048)	.068 (.050)	.016 (.022)	.076 (.069)		1.000 (.561)	.363 (.483)	.104 (.180)
SNP8	.048 (.047)	.249 (.196)	.273 (.178)	.077 (.126)	.349 (.270)	.046 (.015)		.803 (.862)	.290 (.088)
SNP9	.063 (.054)	.070 (.091)	.031 (.065)	.238 (.397)	.000 (.019)	.065 (.065)	.061 (.130)		.283 (.443)
SNP10	.003 (.005)	.013 (.018)	.009 (.003)	.001 (.000)	.008 (.004)	.005 (.008)	.017 (.001)	.007 (.005)	

The diagonal upper right part shows standardized D' in control (bipolar) group between two markers calculated by the COCAPHASE program. The lower left part of diagonal shows r^2 (squared correlation coefficient) in control (bipolar) for bi-allelic marker pairs, and squared values of Cramer's coefficient for pairs with the multi-allelic marker, IVS0-30(GTTTT)$_{4-7}$. NCAM1, neural cell adhesion marker 1; SNP, single nucleotide polymorphism.
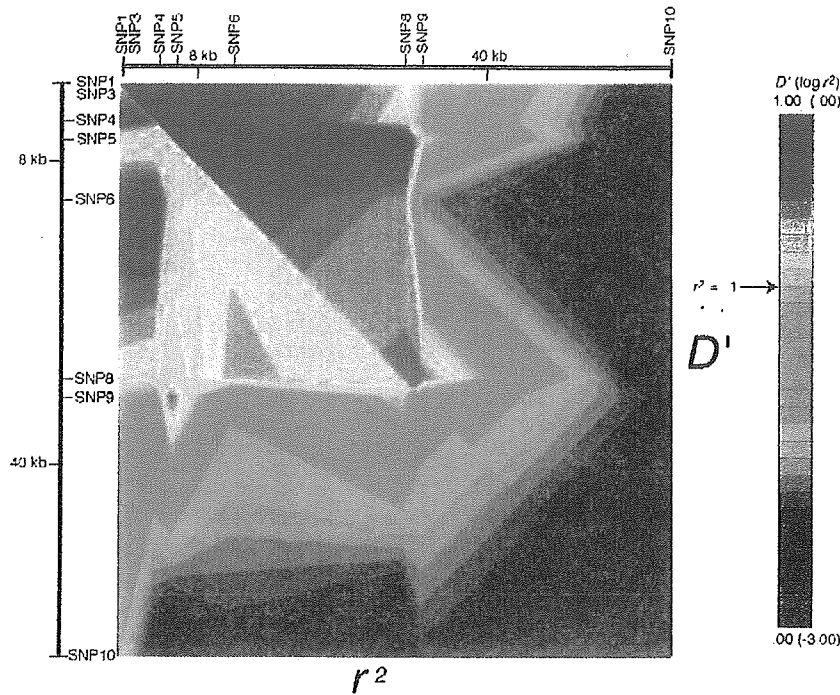
Figure 2. Linkage disequilibrium (LD) map of the NCAM1 locus. Gold plot of color-coded, pairwise disequilibrium statistics (r^2 in diagonal bottom left and D' in diagonal upper right) is shown. Red and yellow indicate areas of strong LD. For single nucleotide polymorphism (SNP) numbers, see Figure 1.

compared with those of control subjects (Vawter et al 1998, 1999). The VASE exon is thought to play functional roles in the modulation of neurite growth activity (Doherty et al 1992). Use of the SEC exon resulted in premature termination of the coding sequence and production of a truncated NCAM polypeptide in brains (Gower et al 1988). IVS7+11G>C is upstream of the VASE exon, and the IVS12+21C>A variant is upstream of the alternatively spliced small exons and SEC exon. Examination of the correlation between NCAM1 genotypes and the content of alternatively spliced exons in bipolar brains would therefore be

intriguing. We recently demonstrated just such a genotype (polymorphic repeats in a gene promoter region)-phenotype (expression level of gene product in postmortem brains) in a study of the N-methyl-D-aspartate receptor NR2A subunit gene (Itokawa et al 2003).

NCAM1 displayed a significant association with bipolar disorder but not with unipolar disorder. Power analysis showed that the size of our unipolar sample had adequate power to detect a relative risk of more than 2.0 but might miss small gene effects (relative risk < 1.5). Nevertheless, the failure to discern an

Figure 3. Results of three-marker and nine-marker haplotype analyses in bipolar samples. For three-marker analysis, a sliding window of three markers was tested, with two-marker overlaps. Below each over-represented haplotype is the p value for that haplotype. "Global (P value)" represents the overall significance when the observed versus expected frequencies of all of the haplotypes are considered together. "Individual Haplotype (P value)" represents significance of the deviated distribution of the risk haplotype in the bipolar group compared with control subjects. The p values were calculated with COCAPHASE (Dudbridge 2002; http://www.hgmp.mrc.ac.uk/~fdudbrid/software/).

Table 5. Estimated Haplotype Frequencies of the NCAM1 Gene

Haplotype SNP1-3-4-5-6-7-8-9[a]	Frequency[b]		
	Bipolar Subjects ($n = 151$)	Control Subjects ($n = 357$)	p^c
Del-1-G-T-G-T-G-A	.0501	.0466	.8044
Del-1-G-T-G-T-G-C	.0268	.0456	.1519
Ins-1-G-T-C-G-T-C	.3241	.2916	.3202
Ins-1-G-T-C-G-G-C	.0570	.0547	.8936
Ins-1-G-C-C-G-G-A	.1472	.0883	.0086
Ins-1-G-C-C-G-G-C	.0381	.0493	.4416
Ins-1-C-T-G-G-G-C	.0000	.0146	.0087
Ins-2-C-T-G-G-T-C	.0255	.0240	.8938
Ins-2-C-T-G-G-G-C	.1004	.1136	.5520
Ins-3-C-T-G-G-G-A	.0296	.0158	.2011
Ins-3-C-T-G-G-G-C	.1417	.2043	.0229
Ins-4-C-T-G-G-G-A	.0109	.0112	.9128
Ins-4-C-T-G-G-G-C	.0486	.0406	.6353
Global p value[c]			.0326

NCAM1, neural cell adhesion molecule 1; SNP, single nucleotide polymorphism.

[a]SNP1, allele Del = deletion, allele Ins = insertion; SNP3, allele 1 = $(GTTTT)_4$, allele 2 = $(GTTTT)_5$, allele 3 = $(GTTTT)_6$, allele 4 = $(GTTTT)_7$.

[b]Haplotpe frequencies were estimated by COCAPHASE.

[c]Calculated by COCAPHASE

association with unipolar disorder might not be due to the smaller statistical power of the analysis compared with bipolar disorder, because the genotypic and allelic frequencies in unipolar disorder resembled those of control subjects, not subjects with bipolar disorder. The present genetic findings suggest that the role of NCAM1 is pathophysiologically more relevant to bipolar disorder than to unipolar disorder. Such a result is in line with the aforementioned reports on NCAM1 perturbation in bipolar disorder (Vawter et al 1998, 1999) and might be in line with reports on disturbed brain histopathology in bipolar disorder (Bouras et al 2001; Rajkowska et al 2001). Other recent studies have also demonstrated pathophysiologic distinctions between bipolar and unipolar depression (Beyer and Krishnan 2002; Cotter et al 2001; Ongur et al 1998; Vawter et al 2000b).

In conclusion, our data suggest the possible involvement of human *NCAM1* or a nearby gene in vulnerability to bipolar affective disorder.

Abecasis GR, Cookson WO (2000): GOLD-graphical overview of linkage disequilibrium. *Bioinformatics* 16:182-183.

Abecasis GR, Noguchi E, Heinzmann A, Traherne JA, Bhattacharyya S, Leaves NI, et al (2001): Extent and distribution of linkage disequilibrium in three genomic regions. *Am J Hum Genet* 68:191-197.

American Psychiatric Association (1994): *Diagnostic and Statistical Manual of Mental Disorders, 4th ed.* Washington, DC: American Psychiatric Press.

Barton CH, Dickson G, Gower HJ, Rowett LH, Putt W, Elsom V, et al (1988): Complete sequence and in vitro expression of a tissue-specific phosphatidylinositol-linked N-CAM isoform from skeletal muscle. *Development* 104:165-173.

Berrettini WH (2000): Are schizophrenic and bipolar disorders related? A review of family and molecular studies. *Biol Psychiatry* 48:531-538.

Berrettini WH (2001): Molecular linkage studies of bipolar disorders. *Bipolar Disord* 3:276-283.

Berrettini W (2002): Review of bipolar molecular linkage and association studies. *Curr Psychiatry Rep* 4:124-129.

Beyer JL, Krishnan KR (2002): Volumetric brain imaging findings in mood disorders. *Bipolar Disord* 4:89-104.

Bouras C, Kovari E, Hof PR, Riederer BM, Giannakopoulos P (2001): Anterior cingulate cortex pathology in schizophrenia and bipolar disorder. *Acta Neuropathol* 102:373-379.

Cardno AG, Marshall EJ, Coid B, Macdonald AM, Ribchester TR, Davies NJ, et al (1999): Heritability estimates for psychotic disorders: The Maudsley twin psychosis series. *Arch Gen Psychiatry* 56:162-168.

Cotter D, Mackay D, Landau S, Kerwin R, Everall I (2001): Reduced glial cell density and neuronal size in the anterior cingulate cortex in major depressive disorder. *Arch Gen Psychiatry* 6:545-553.

Craddock N, Dave S, Greening J (2001): Association studies of bipolar disorder. *Bipolar Disord* 3:284-298.

Craddock N, Jones I (1999): Genetics of bipolar disorder. *J Med Genet* 36:585-594.

Cremer H, Lange R, Christoph A, Plomann M, Vopper G, Roes J, et al (1994): Inactivation of the N-CAM gene in mice results in size reduction of the olfactory bulb and deficits in spatial learning. *Nature* 367:455-459.

Doherty P, Moolenaar CE, Ashton SV, Michalides RJ, Walsh FS (1992): The

VASE exon downregulates the neurite growth-promoting activity of NCAM 140. *Nature* 356:791-793.

Dudbridge F (2002): Methods and software for association tests of uncertain haplotypes in case-parent trios. *Am J Hum Genet* 71(suppl):A2338.

First MB, Spitzer RL, Gibbon M (1997): *Structured Clinical Interview for DSM-IV Axis I Disorders (Clinician Version).* Washington, DC: American Psychiatric Press.

Goridis C, Brunet JF (1992): NCAM: Structural diversity, function and regulation of expression. *Semin Cell Biol* 3:189-197.

Gower HJ, Barton CH, Elsom VL, Thompson J, Moore SE, Dickson G, et al (1988): Alternative splicing generates a secreted form of N-CAM in muscle and brain. *Cell* 55:955-964.

Hutton M, Lendon CL, Rizzu P, Baker M, Froelich S, Houlden H, et al (1998): Association of missense and 5'-splice-site mutations in tau with the inherited dementia FTDP-17. *Nature* 393:702-705.

Itokawa M, Yamada K, Yoshitsugu K, Toyota T, Suga T, Ohba H, et al (2003): A microsatellite repeat in the promoter of the N-methyl-D-aspartate receptor 2A subunit (GRIN2A) gene suppresses transcriptional activity and correlates with chronic outcome in schizophrenia. *Pharmacogenetics* 13:271-278.

Kato T (2001): Molecular genetics of bipolar disorder. *Neurosci Res* 40:105-113.

Kiss JZ, Muller D (2001): Contribution of the neural cell adhesion molecule and synaptic plasticity. *Rev Neurosci* 12:297-310.

Mendlewicz J, Rainer JD (1977): Adoption study supporting genetic transmission in manic-depressive illness. *Nature* 268:327-329.

Nakajima T, Jorde LB, Ishigami T, Uemura S, Emi M, Lalouel J-M, et al (2002): Nucleotide diversity and haplotype structure of the human angiotensin gene in two populations. *Am J Hum Genet* 70:108-123.

Ongur D, Drevets WC, Price JL (1998): Glial reduction in the subgenual prefrontal cortex in mood disorders. *Proc Natl Acad Sci U S A* 95:13290-13295.

Poltorak M, Frye MA, Wright R, Hemperly JJ, George MS, Pazzaglia PJ, et al (1996): Increased neural cell adhesion molecule in the CSF of patients with mood disorder. *J Neurochem* 66:1532-1538.

Rajkowska G, Halaris A, Selemon LD (2001): Reductions in neuronal and glial density characterize the dorsolateral prefrontal cortex in bipolar disorder. *Biol Psychiatry* 49:741-752.

Ronn LC, Hartz BP, Bock E (1998): The neural cell adhesion molecule (NCAM) in development and plasticity of the nervous system. *Exp Gerontol* 33:853-864.

Saito S, Tanio Y, Tachibana I, Hayashi S, Kishimoto T, Kawase T (1994): Complementary DNA sequence encoding the major neural cell adhesion molecule isoform in a human small cell lung cancer cell line. *Lung Cancer* 10:307-318.

Sham PC, Curtis D (1995): Monte Carlo tests for associations between disease and alleles at highly polymorphic loci. *Ann Hum Genet* 59:97-105.

Taylor L, Faraone SV, Tsuang MT (2002): Family, twin, and adoption studies of bipolar disease. *Curr Psychiatry Rep* 4:130-133.

Tomasiewicz H, Ono K, Yee D, Thompson C, Goridis C, Rutishauser U, et al (1993): Genetic deletion of a neural cell adhesion molecule variant (N-CAM-180) produces distinct defects in the central nervous system. *Neuron* 11:1163-1174.

van Duijnhoven HL, Helfrich W, de Leij L, Roebroek AJ, van de Ven WJ, Healey K, et al (1992): Splicing of the VASE exon of neural cell adhesion molecule (NCAM) in human small-cell lung carcinoma (SCLC). *Int J Cancer* 50:118-123.

Vawter MP (2000a): Dysregulation of the neural cell adhesion molecule and neuropsychiatric disorders. *Eur J Pharmacol* 405:385-395.

Vawter MP, Freed WJ, Kleinman JE (2000b): Neuropathology of bipolar disorder. *Biol Psychiatry* 48:486-504.

Vawter MP, Hemperly JJ, Hyde TM, Bachus SE, VanderPutten DM, Howard AL, et al (1998): VASE-containing N-CAM isoforms are increased in the hippocampus in bipolar disorder but not schizophrenia. *Exp Neurol* 154:1-11.

Vawter MP, Howard AL, Hyde TM, Kleinman JE, Freed WJ (1999): Alterations of hippocampal secreted N-CAM in bipolar disorder and synaptophysin in schizophrenia. *Mol Psychiatry* 4:467-475.

Short Communication

Identification of a male schizophrenic patient carrying a de novo balanced translocation, t(4; 13)(p16.1; q21.31)

MASANARI ITOKAWA, MD,[1,2] TAKEHIKO KASUGA, MD,[3] TAKEO YOSHIKAWA, MD[2] AND MASAAKI MATSUSHITA, MD[3,4]

[1]*Department of Schizophrenia Research,* [4]*Tokyo Institute of Psychiatry,* [3]*Department of Psychiatry, Tokyo Metropolitan Matsuzawa Hospital, Setagaya, Tokyo and* [2]*Laboratory for molecular Psychiatry, RIKEN Brain Science Institute, Wako, Saitama, Japan*

Abstract   Herein is reported the case of a male patient with schizophrenia who displayed a de novo balanced translocation between the short arm of chromosome 4 and the long arm of chromosome 13, t(4; 13)(p16.1; q21.31). The 4p16.1 region is where the causative gene (*WFS1*) for Wolfram syndrome has been mapped. In Wolfram syndrome, approximately 60% of patients suffer from major mental illness. The other breakpoint, chromosome 13q21.31, is another region where previous linkage studies have repeatedly detected linkage to schizophrenia. The documentation of the present case could therefore provide a valuable resource for identifying disease susceptibility genes by localizing the breakpoints.

Key words: chromosome 4, chromosome 13, cytogenetic abnormality, karyotype, GTG-banding, Wolfram syndrome.

INTRODUCTION

Evidence from family, twin and adoption studies has suggested the existence of important genetic contributions to the etiology of schizophrenia.[1] Linkage and association studies often yield valuable, but sometimes conflicting, results for schizophrenia, and the responsible genes have proven difficult to isolate.[2] An alternative to these genetic approaches would be the identification and precise genomic analysis of chromosomal abnormalities that are cosegregated with the disease. MacIntyre *et al.* compiled a list of translocations coexisting with mental illnesses and tried to assess the relevance of these to diseases based on three criteria.[3] These criteria were (i) rarity of the translocation and independent reports of coexistence of the translocation with psychiatric illness; (ii) colocalization of the abnormality with suggestive linkage findings; and (iii) coseg-

regation of the abnormality with illness within a family. Analysis of a chromosomal aberration fulfilling all three criteria, a t(1; 11)(q42.2; q14.3) translocation identified in a Scottish family suffering from major psychiatric illnesses, led to the isolation of genes *disrupted-in-schizophrenia-1* and *-2* (*DISC1* and *DISC2*).[4]

We report herein the case of a male patient with schizophrenia who displayed a de novo balanced translocation between chromosomes 4 and 13, and discuss the usefulness of this case for molecular dissection of schizophrenia susceptibility genes.

CASE REPORT

Clinical course

The proband was a 42-year-old man who was the second child of unrelated parents. He was born at term after an uneventful pregnancy and normal delivery. Psychomotor development was normal. After graduating from high school at 18 years of age, he was employed by a company. Thereafter, he changed jobs every 1–2 years. From around 30 years of age he began to manifest alcohol-related problems, such as violence against his parents while intoxicated. At 37 years of age

Correspondence address: Dr Masanari Itokawa, Department of Schizophrenia Research, Tokyo Institute of Psychiatry, 2-1-8 Kamikitazawa, Setagaya, Tokyo 156-8585, Japan. Email: mitokawa@prit.go.jp

he borrowed 2000 000 yen from his father and went to the USA in an attempt to set up a business. However, 3 months later he returned to Japan without any business success and started to live alone in an apartment. At 38 years of age he began to exhibit insomnia, psychomotor excitement, and persecutory delusion, and was admitted to a psychiatric hospital.

He was 170 cm tall and weighed 60 kg. Neurological examination and computed tomography of the brain revealed no abnormalities. Laboratory tests identified renal abnormality, and ultrasonography detected polycysts in the left kidney and stones in the right. He suffered from bizarre delusions of being influenced by external forces ('Government has put a microchip in my brain to control all of my behavior, read my thought and inform everybody of my private thoughts'). Although not prominent, disorganized speech was also noted, with the patient moving quickly from one topic to another. Based on the consensus of two experienced psychiatrists in non-structural psychiatric interviews, family information and all available medical records, a diagnosis of paranoid schizophrenia was made according to *Diagnostic and Statistical Manual of Mental Disorders* (4th edn; DSM-IV) criteria. Psychotic symptoms responded well to treatment with resperidon. The Positive and Negative Symptom Scale (PANSS)[5] was examined in the remission state after treatment, giving scores of 9 on positive symptoms, 13 on negative symptoms, and 29 on general non-psychotic psychiatric symptoms.

Family history

Non-structural detailed interviews of family members by two experienced psychiatrists, revealed no suggestion of psychiatric illness among individuals within the second-degree relatives of the proband (Fig. 1). Of the seven siblings of the proband's father, three sisters (05, 06 and 11) suffered from diabetes mellitus, and a brother (09) had been blind since 6 years of age, although the cause was unknown. The mother (18) suffered from hypertension and diabetes mellitus, and both her brother (16) and mother (04) displayed histories of renal disease (precise diagnoses unknown).
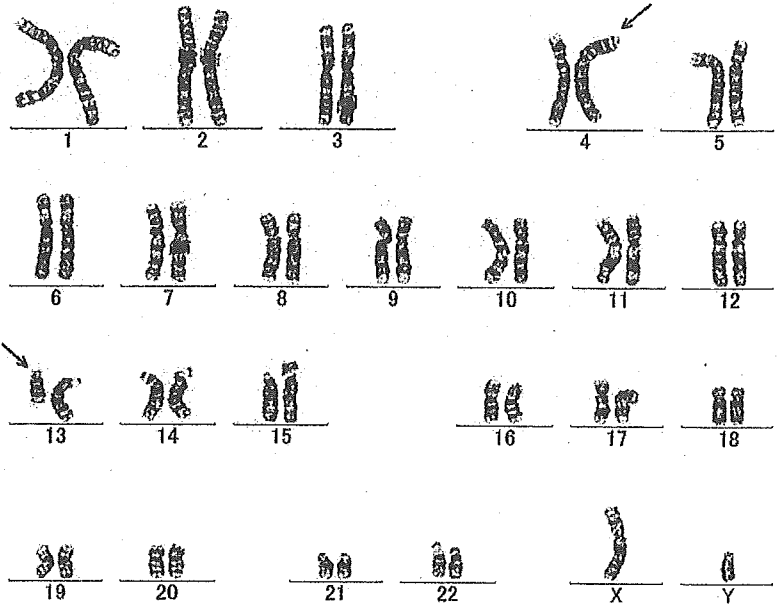
Cytogenetic findings

High-resolution karyotyping of GTG-banded chromosomes (850 band level) in the patient demonstrated a balanced translocation between band p16.1 of chromosome 4 and band q21.31 of chromosome 13 in each of the 30 lymphocytes examined (Figs 2,3). Karyotype was thus considered to be 46,XY,t(4;13)(p16.1; q21.31). Neither parent displayed any cytogenetic abnormalities, with karyotypes of 46,XY and 46,XX, respectively.

The present study was approved by the Ethics Committees of the Tokyo Institute of Psychiatry and Matsuzawa Hospital, and all participants provided written informed consent.
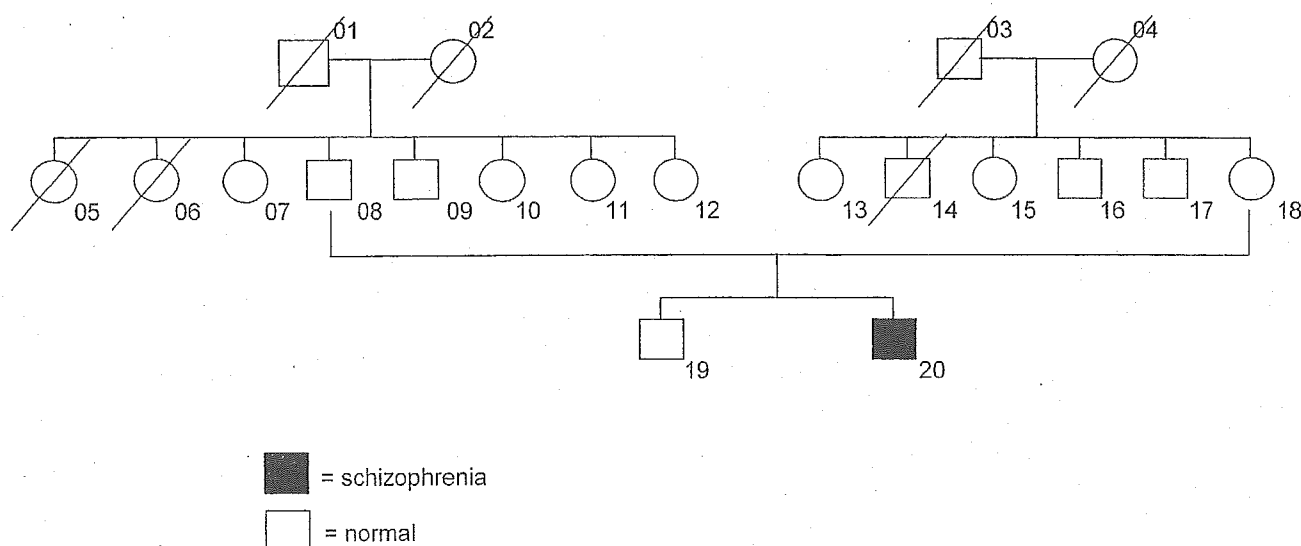
Figure 1. Family structure and psychiatric phenotype. Individual 20 displayed a chromosomal abnormality, while both parents demonstrated normal karyotypes.

Figure 2. Karyotype of individual 20. Balanced translocation between 4p and 13q is illustrated, 46,XY,t (4;13) (p16.1; q21.31).
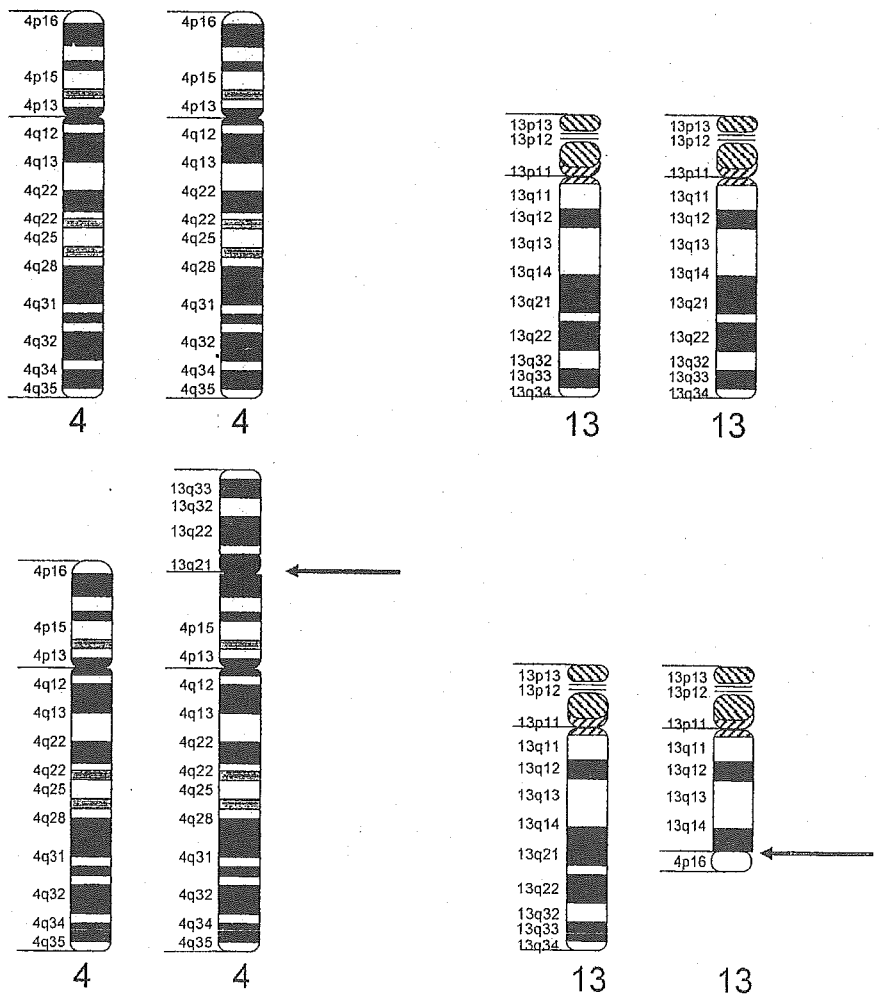
Figure 3. Diagram showing normal chromosomes 4 and 13 (top) and cytogenetic interpretation of the breakpoints (arrow) involved in the translocation (below).